View metadata, citation and similar papers at core.ac.uk

brought to you by CORE

provided by AFTI Scholar (Air Force Institute of Technology)

Air Force Institute of Technology

AFIT Scholar

Theses and Dissertations | Student Graduate Works

6-2005

Categorizing High Energy Laser Effects for the Joint Munitions Effectiveness Manual

James A. Markham

Follow this and additional works at: https://scholar.afit.edu/etd

Part of the Other Operations Research, Systems Engineering and Industrial Engineering Commons, and the Risk Analysis Commons

Recommended Citation

Markham, James A., "Categorizing High Energy Laser Effects for the Joint Munitions Effectiveness Manual" (2005). *Theses and Dissertations*. 3778.
https://scholar.afit.edu/etd/3778

This Thesis is brought to you for free and open access by the Student Graduate Works at AFIT Scholar. It has been accepted for inclusion in Theses and Dissertations by an authorized administrator of AFIT Scholar. For more information, please contact richard.mansfield@afit.edu.

CATEGORIZING HIGH ENERGY LASER EFFECTS FOR THE JOINT MUNITIONS EFFECTIVENESS MANUAL

THESIS

James A Markham, Captain, USAF

AFIT/GOR/ENS/05-11

DEPARTMENT OF THE AIR FORCE
AIR UNIVERSITY

AIR FORCE INSTITUTE OF TECHNOLOGY

Wright-Patterson Air Force Base, Ohio

APPROVED FOR PUBLIC RELEASE; DISTRIBUTION UNLIMITED

The views expressed in this thesis are those of the author and do not reflect the official policy or position of the United States Air Force, Department of Defense, or the U.S. Government.

AFIT/GOR/ENS/05-11

CATEGORIZING HIGH ENERGY LASER EFFECTS FOR THE JOINT MUNITIONS EFFECTIVENESS MANUAL

THESIS

Presented to the Faculty

Department of Operational Sciences

Graduate School of Engineering and Management

Air Force Institute of Technology

Air University

Air Education and Training Command

In Partial Fulfillment of the Requirements for the

Degree of Master of Science in Operations Research

James A. Markham, BS

Captain, USAF

June 2005

APPROVED FOR PUBLIC RELEASE; DISTRIBUTION UNLIMITED

AFIT/GOR/ENS/05-11

CATEGORIZING HIGH ENERGY LASER EFFECTS FOR THE JOINT MUNITIONS EFFECTIVENESS MANUAL

James A. Markham, BS

Captain, USAF

Approved:

____________________________________ ________

Dr. John O. Miller (Chairman) Date

____________________________________ ________

Robert Brigantic, Lt Col, USAF (Member) Date

AFIT/GOR/ENS/05-11

Abstract

With the high risk and cost in fielding High Energy Laser (HEL) weapon systems, the development process must include computer simulation models of weapon system performance from the engineering level up to predicting the military worth of employing specific systems in a combat scenario. This research effort focuses on defining how to measure lethality for HEL weapons in an Advanced Tactical Laser (ATL) scenario. In order to create an effective measure for direct comparison between the emerging laser weapon system and existing conventionally delivered weapons, lase time in seconds is presented as a measure comparable to rounds required to cause the desired effect at the target. An examination of input parameters which influence the output power of the laser at the target and thus the required lase time is presented with particular attention being paid to atmospheric conditions and vulnerable bucket size. Results include output tables providing the lase time required for melt-through of a set of generic truck-type vehicular ground target aimpoints.

Acknowledgments

First and foremost I would like to thank God Almighty for the strength and determination to undertake this work, and for his allowing me to stay here and finish this work after my unfortunate motorcycle mishap last summer. I would also like to like to express my sincere appreciation to my faculty advisor, Dr. J.O. Miller, for his stalwart support and ever diligent guidance of this thesis effort, and his recommendation that I not attempt to join the professional dart tour. The directive yet not dictative oversight was exactly the stimulus I needed to improve my ability to self-motivate and get this thing done. I would like to express my undying gratitude to Lt Col Moshier and Maj Wiley, for their aid and support of my wife during my recovery. Finally, I would like to thank my wife for her love and support during my medical ordeal and for putting up with me as I completed this work.

James A. Markham

.

Table of Contents

List of Figures

Page

List of Tables

Page

TITLE

I. Introduction

Background

In October 2004 the Joint Munitions Effectiveness Manual Effects (JMEM/FX) lethality working group held a meeting concerning a number of lethality issues for multiple weapons systems. Among these were the Advanced Tactical Laser (ATL), the Airborne Laser (ABL), and other lethal and non-lethal directed energy weapon systems. As these technologies mature, we are drawing closer to the coming paradigm shift in weapon engagements and to the realization of effects based operations. Lasers offer significant advantages over conventional systems, including speed of light delivery to distant targets immediately upon detection, with constrained enemy evasion and limited collateral damage (Perram, 2004).

Though they offer advantages, laser weapons are fundamentally different from conventional kinetic-energy based weapons. Along with the aforementioned speed of light delivery comes degradation in effective power with distance. Unlike a dumb bomb or a missile which carries all its energy from the launcher and then ‘exerts’ that energy at or in the vicinity of the target, a laser’s power diminishes proportionally with increased distance between the launcher and the target. This reduction in power necessitates a different approach in developing planning tools for laser weapons, as this effect must be captured in such a way that the planner is able to understand and effectively utilize those tools.

Research Objectives/Questions/Hypotheses

The objective of this research is to develop a methodology for production of JMEM type data for the Advanced Tactical Laser platform. An examination of relevant input factors must be presented, and analysis of which factors may be necessary for consideration in vulnerability prediction must be performed. Relevant questions include: Which input factors are significant in predicting the laser output? Which output measures are most directly applicable to use in calculating target vulnerability? Finally, how does the predicted vulnerability vary with those input factors determined to be significant? It is hypothesized that the major driver in power output prediction will be the distance to the target, given the physical properties of the engagement scenario. It is also hypothesized that the various atmospheres tested will affect the output power, however no predictions are made at this point as to whether various atmospherics will increase or decrease the output power.

Research Focus

This research will focus on the issues surrounding laser weapons and their utilization, specifically propagation through the atmosphere, target and platform engagement geometry, predicted laser power output, and vulnerability based on target thresholds. A number of output measures will be examined in order to determine the best or most representative measure for reliable damage prediction and weapon system comparison.

Methodology

The methodology employed for this research will include data generation by a physics based model, which will output a number of measures of laser energy at the target. The data will then be analyzed in order to assure that the output follows expectation based on the physics of the scenario. The input factors will be analyzed against the outputs to determine which are the driving factors, and then linear regression will be used to predict that output. Finally, target vulnerability will be examined through the use of laser test data, which will be used in conjunction with the predictive model output to generate vulnerability tables for use by the weaponeering community.

Assumptions/Limitations

This research assumes that the ATL system will be fielded as initially projected, and bases the system capability on unclassified system characteristics obtained from the System Program Office (SPO). The propagation model used assumes perfect laser tracking, and median atmospheric characteristics (summer, 50^{th} percentile relative humidity) for each of the atmospheres utilized in laser output calculations.

Implications

The results of this research will be applicable to system effectiveness for the ATL, and will present a capabilities profile for the system. This profile will be usable by a JMEM end user for ATL mission planning, and by a SPO analyst for exploration of ATL

Concept of Operations (CONOPS) determination. The applicability of the research conclusions will be limited by the assumptions listed above, but the research results will be extensible through the utilized methodology when considerations for exploration beyond the initial assumptions are included.

II. Literature Review

Introduction

In order to perform meaningful research for this project, a review of the applicable unclassified literature needs to be performed. One interesting note is that though there may be additional information available in a classified medium, this research is limited to the open source unclassified information available. It is understood that due to the nature of a new weapon system still in development, there are a number of performance characteristics which will be classified until the system is fielded, and some which will remain classified even after the system is operational. It is important therefore to perform a thorough review of the available literature, in order to examine all relevant issues as accurately as possible.

Department of Defense Modeling and Simulation

Modeling and Simulation (M&S) is defined as "The process of designing a model of a system and conducting experiments with this model for the purpose either of understanding the behavior of the system or of evaluating various strategies for the operation of the system" (Shannon). M&S is done within the Department of Defense (DoD) as a means to save resources, such as time, money, personnel, or any combination thereof. Modeling and simulation can be performed when it would be expensive or dangerous to use the real systems. Additionally, a system may be simulated because there is enough inherent variability in the system's processes that an analytic solution to the question being asked may be very messy, extremely taxing computationally, or completely intractable. A model is a representation of a system and a simulation is a utilization of a model; however, for the remainder of this thesis, these two terms are used interchangeably.

Model Hierarchy

Within the realm of DoD M&S, models and simulations are classified by the level of warfare they model. This classification is traditionally depicted as a pyramid, with the higher fidelity, higher resolution models concerned with lower levels of warfare at the bottom, and the strategic level models at the top.

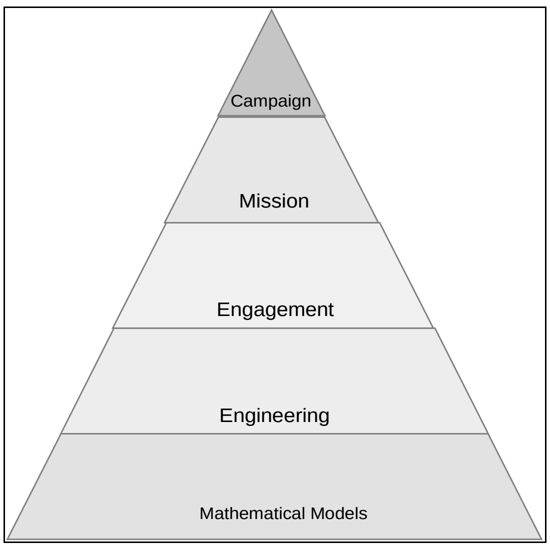

Figure 1: DoD M&S Pyramid

At the bottom are the mathematical models, which are used to explicitly describe processes, e.g. physics equations describing the ballistics of a projectile in flight. Examples of models at this level are Newton's laws of motion, and the like. The second level consists of engineering level models which combine a number of mathematical models to describe a series of events where the level of warfare is at the system vs. system level. An example of this would be the interaction of a given rifle round with a particular type of body armor. Next on the way up the pyramid are the Engagement level models, which move from system vs. system to platform vs. platform, with each platform consisting of a number of individually described systems. At this level, the physics equations for a round being fired may be reduced to a simple muzzle velocity, which suffices for a description of the firing process at this level of resolution. These models operate at the operational level of warfare, where tactics, techniques, and procedures are modeled using rule sets governing the behavior of systems with regard to events within the simulation. At the fourth level are the mission level models which move from 1 vs. 1 to Many vs. Many with regard to numbers of platforms involved. At the top of the pyramid are the campaign level models, which describe operations at the theater and strategic levels of warfare. These models utilize inputs concerning the actions of large groups of systems and their interaction within the framework of a large battlespace. In general, the aggregation increases as one moves up the pyramid, and fidelity increases as one moves down, but this is not always the case. The primary model used in this research effort, the High Energy Laser End to End Operational Simulation (HELEEOS), is primarily an engagement level model, and will be described in detail later in this literature review.

Joint Munitions Effectiveness Manual

Now that we have explored the range of models available for analyst evaluation of operational scenarios, it is important to understand the specific output required by the end user in the field. Planners and targeteers operate in an environment where the use of a combat model to give a point prediction for weapon effectiveness, or the time required to perform a large number of replications in order to form a tighter prediction are not conducive to completing work in a timely manner. The operational environment for a planner requires that any estimates they use for targeting purposes are as simple as looking a value up in a table given the scenario for a particular target engagement. This requires that a great deal of work has been done by the analysis community to accurately populate those tables, and to make sure that the tables are based on the correct factors for the scenarios involved.

Manual Basics

The Joint Munitions Effectiveness Manual (JMEM) comprises a series of Field Manuals (FM) which describe the capabilities of weapons systems against different targets based on the profile by which the weapon is delivered. Unfortunately for the academic, these documents are classified due to the nature of the data they contain. Additionally, very little information is available in the unclassified arena concerning the generation, formatting, and use of this data. However, one can establish a methodology for developing the data, and through the use of unclassified or notional data, can verify and validate that methodology as an acceptable data production tool. With the validated methodology in hand, one can produce relevant output once the ‘correct’ inputs are linked up with the tool. In order to generate this methodology, it is necessary to identify exactly the area of combat to which the data will be applied, and to present the data in as similar a format to existing data for that field as is possible.

Lethality, Probability of Kill

For the purposes of this thesis we define the Probability of Effectiveness (P_{eff}) as the probability that the given set of input criteria will produce a result such that the desired effect is reached. Traditionally in the directed energy forum, there has been a misconception about JMEM in that there is some mythical P_k or Probability of Kill whereby the targeteer is able to divine the required number of weapons to utilize in order to effectively neutralize the chosen target. In actuality, the primary measure of effectiveness used in JMEM data is the ability to cause one of the following desired effects: Delay, Disable, or Destroy. Modelers have had to develop rulesets for engagements and in order to capture the effect of a near-miss have created the concept of mobility kills, firepower kills, and catastrophic kills. This modeling construct has unfortunately bled back over into the community's perception of the real world data.

Though the set of Measures of Effectiveness (MOEs) for Lasers may be similar to or contain some of the same elements as those for kinetic weapons, they have not as yet been defined. As has been previously mentioned, laser power decreases over distance. This is one of the fundamental differences between kinetic and beam weapons, and therefore demands that we include it in our discussion of MOEs. Where there are a single set of values for damage given by a kinetic weapon, the dependence on a direct hit and associated dwell time may dictate a graduated list of values for lasers, based on lase time as an analog to the number of rounds used in a traditional kinetic scenario.

Little work has been directed toward developing and circulating a methodology for determining lethality or the thresholds for differing levels of non-lethal effects. While kinetic weapons may deliver their full energy in the vicinity of their target and thus cause less than complete kill effects, a laser shot is either a hit or a miss. The laser however can hit the target and ‘quit’ delivering energy when a specified level of damage has been administered, allowing for tailored effects through the use of the same weapon. (Dial-a-Damage, as was opined by one of the JMEM/FX meeting attendees). This research will attempt to establish an initial methodology for development of lethality data for use in planning and modeling tools.

Laser Issues

We cannot adequately discuss the use of lasers in combat without reviewing the literature on the initial development of lasers and their subsequent advancements toward weaponization. We must cover both the work done to develop lasers with more output power and with better propagation characteristics. Additionally, we need to cover the development of optics used in the aiming and targeting of laser systems, as these developments have a significant impact on the applicability of laser systems to military objectives.

Weaponized lasers

The LASER, which stands for Light Amplification by Stimulated Emission of Radiation, was originally developed by Shawlow and Townes at Bell Labs in 1958 as an extension to MASER (Microwave Amplification by Stimulated Emission of Radiation) technology developed a few years earlier. The acronym for a LASER has become part of common speech, with the Merriam-Webster dictionary defining a laser as "a device that utilizes the natural oscillations of atoms or molecules between energy levels for generating coherent electromagnetic radiation usually in the ultraviolet, visible, or infrared regions of the spectrum".

The US Navy has been working on High Energy Laser (HEL) technologies since the early 70's, with the advent of Deuterium Fluoride (DF) lasers. Earlier developments in CO_2 lasers offered a laser which did not propagate in the sea-level maritime atmosphere nearly as well as the newly developed DF lasers (Albertine, 2002). The Navy-ARPA Chemical Laser (NACL) was successful at engaging and destroying high-subsonic TOW missiles in flight in March of 1978. Citing DoD over-emphasis on long wavelength IR laser technology, Congress cancelled the Sea Lite program under which the NACL and the follow-on Mid-Infrared Advanced Chemical Laser (MIRACL) in 1983. Congress failed to notice that for projected laser engagement scenarios (sea level, <10km range) the propagation for the IR lasers was better than the Chemical Oxygen-Iodine Laser (COIL) systems. Laser integration with a tracking system was continued in order to gain the engineering experience with an established laser while waiting on the development of newly directed technology. This integration culminated with the successful shootdown of a VANDAL supersonic missile by the MIRACL system in 1989, and follow-on testing to improve weapon accuracy through improved beam aiming systems and jitter reduction.

The Air Force Weapons Lab has also been working on HEL technology, with early work beginning in the 1970's. The Air Force Research Lab (AFRL) first demonstrated a COIL in 1977 (Perram 2004). The military applicability of airborne lasers was first championed in 1967 by Edward Teller. His idea culminated in the development of the Airborne Laser Laboratory (ALL) which was a KC-135 Aircraft modified to carry a carbon dioxide gas dynamic laser. This system succesfully shot down two towed drones and a number of sidewinder air to air missiles at the White Sands Missile Range, New Mexico in May of 1981 (Boeing, 2001).

In November 1996, Congress authorized Boeing, Northrop Grumman, and Lockheed Martin to begin development of the successor to the ALL, the Airborne Laser (ABL). Based on the much larger 747-400 and using a COIL laser much more powerful than the ALL's gas dynamic laser, the ABL was developed to intercept and destroy theater ballistic missiles in their boost phase. A smaller COIL laser system has also been developed for Special Operations Command (SOCOM), for use in support of ground operations. The ATL system carries a one-hundred kilowatt laser in the fuselage of a C-130 aircraft, and projects the beam from a turret mounted underneath the aircraft. A more detailed description of this system follows later, as it is the weapon selected for study in this research effort.

Propagation

As has been stated above, one of the primary concerns with evaluating the effectiveness of a laser system is the proportional loss of system power with increasing distance from the platform to the target. There are a number of ways of determining this resultant loss in power, each having its advantages and disadvantages. Captain Azar's (2003) work used a first order brightness equation scaled by a factor of $1/R^2$ where R is the distance from the target. This gave a resulting power reaching the target in watts per square meter. There are currently a number of much more detailed sets of calculations known as wave optics codes which use detailed physics equations for optics and the propagation of light to represent the travel of a laser beam through various atmospheric effects. Among these are Science Applications International Corporation's (SAIC's) Atmospheric Compensation Simulation (ACS) code and MZA Associates Corporation's WaveTrain code. Both of these represent the current pinnacle in laser propagation fidelity and accuracy; however they both have extremely high computational overhead, with runs taking on the order of several hours. This amount of time for propagation calculation will definitely not be available to the operator in the field, thus we need a faster way to describe the 'flyout' of the laser. Though they are not developed with the same level of fidelity as the wave optics codes, scaling law models such as HELEEOS are orders of magnitude faster with run times on the order of seconds instead of hours.

Developed by the Air Force Institute of Technology Center for Directed Energy under the sponsorship of the HEL Joint Technology Office (JTO), HELEEOS is being designed to provide reasonable fidelity in predictions of energy delivered to a target for a wide range of militarily applicable input parameters (HELEEOS User's Guide). The output from HELEEOS has been benchmarked and tuned to match up with the output of the ACS code at a number of design points. This assists in validating the output of HELEEOS by assuring the user that for a given set of inputs, the output of the scaling law model will reasonably match up with the output of a higher fidelity model. Currently the HELEEOS model has a number of limitations, such as the lack of adaptive optics and a 'top hat' profile for beam intensity. However, since the area of laser weapon adaptive optics is still a developing field, and this work is concerned with the intensity over time and not specifically at any given point, neither of these are identified as limiting factors with regard to this research effort. The model does support dynamic engagements where the platform and target move relative to each other over the course of the laser engagement. Since the scenario used for this work will implement C-130 Gunship employment methodology, the relative geometry should remain almost constant for the duration of any given engagement.

Targeting

One problem associated with the implementation of an ultra-precise weapon system on board an aircraft in flight is the ability to accurately designate and lock onto targets at an extended distance. Though the projected laser system can project lethal fluence to distances somewhere in excess of 20 kilometers, the ability to accurately pick out a target and aim the laser at that distance is lacking. This is analogous to a readily understandable and well established ground based kinetic weapon problem. The standard issue M1903 Springfield battle rifle used during WWI by U.S. troops was accurate at ranges out to 1000 yards, but until the addition of optical sights, the effective range of the weapon was only 600 yards. Just as the .30-06 round accurately carries a lethal amount of energy beyond the ~600 yard sight range of the common soldier, the ATL beam still retains sufficient brightness to effect damage out past the range of the current sighting optics. This also means that with improved sighting optics and aiming components, it may be possible to also extend the effective range of the ATL as was done with the M1903.

Another problem arising from the addition of laser weapons to an arsenal stems from their stark contrast to the traditional kinetic weapon systems which operators are trained on and familiar with. The ATL will at least initially come online as a Special Operations Command (SOCOM) weapon, filling a new niche very close to that currently occupied by the UC-130 Spectre gunship. The instantly apparent difference in these two systems is the level of operator feedback involved in their associated weapon systems. While the Spectre provides instant feedback in the form of rounds visibly striking (or missing) a target, and the resultant payload reaction (high explosive, incendiary, etc), the ATL may not provide this level of feedback. At extended engagement ranges, the operator will have to be able to trust that the system performed as desired, and will have to be able to do so automatically. It is beyond the capability and outside the job description of a weapons officer to require them to calculate necessary fluence on target and the corresponding amount of lase time required to attain that level of fluence. This functionality will need to be built into the targeting computer system, such that the operator will simply select the target from a pre-loaded list and when the trigger is pulled, the appropriate lase time will occur automatically. Also, since SOCOM is well known for ‘inventive’ uses of systems, the targeting computer will need a large collection of generic targets for an operator to choose from in order to deal with emergent situations.

Design of Experiments / Linear Regression / ANOVA

In order to evaluate the data output from the model, we can use any one of a number of analysis techniques. Because no one technique is the be-all, end-all tool for data analysis, it is advisable to look at the data using at least a few of the most applicable techniques for the particular data set.

Design of experiments (DOE) refers to the particulars of an experiment, including the treatments, experimental units, rules and procedures for assigning treatments to experimental units, and measurements on the experimental units following treatment application (Neter, 1996). In general, DOE is most concerned with the rules and procedures portion of the aforementioned list, in order to maximize efficiency. Sir R.A. Fisher introduced the concept of randomization for experimental treatment application as a means of eliminating bias. By randomly selecting the order in which the treatments are applied, any systemic or subjective bias is effectively reduced or removed. This randomization is only necessary to remove unknown bias from the system, and is not necessary in the case of deterministic computer models, as each run is independent of run order, and will produce the same output whether the run is first, last or anywhere in the middle of a large run set.

Linear regression is the method of using a number of input variables and their relationship to an associated response variable to construct a linear model with which the output or response variable can be predicted based on a given set of inputs. As an example, for this particular problem we know that the output power of the laser decreases with increased distance, so the an increase in the distance input variable would have a negative impact on the power output response. The end result is a fixed equation into which the input variables are substituted in order to predict the output with negligible computational expense.

ANOVA stands for Analysis of Variance, which is another method of studying the relation between a response variable and the associated input or explanatory variables. ANOVA models do not require any statistical assumptions about the nature of the explanatory variables, nor do they require those variables to be strictly quantitative. Again, as an example, given that the geographic factor for laser output power is a qualitative variable, it follows that an ANOVA model would be developed in order to aid in the construction of the regression model. Should two levels of the geographic factor be shown to be statistically different, it would follow that they should use different regression equations to model the power output. On the other hand, should they be shown to not be statistically different, then we would be justified in using the same regression model for both of the factor levels.

Advanced Tactical Laser System

Overview

The Advanced Tactical Laser weapon system consists of a C-130 aircraft containing a sealed-exhaust Chemical Oxygen-Iodine Laser (COIL) with a laser turret mounted underneath the fuselage. The turret will be retractable for takeoff and landing in order to avoid modification of the landing gear. The current development contract is held by Boeing and though a variant system was originally being envisioned for use with the MV-22 Osprey airframe, the current incarnation of the system is limited to the C-130.

The system is limited in output by the airlift capacity of the chosen airframe. In comparison, the 747-400 based Airborne Laser (ABL) has a much larger payload capacity, and thus it carries a larger laser, with power output in the megawatt class.

Concept of Operations

The ATL is one of the first in a new class of ultra-precision weapon systems which will change the face of the modern battlefield. The ability to interdict over long range with pinpoint accuracy brings a large capability to the fight. In addition to the weapon platform itself, the system brings a highly capable intelligence gathering tool in the form of the laser sighting optics. The ability to maintain a laser spot on a target at range is predicated on the capability to see and distinguish targets at range. This long range 'observer' role is a force multiplier for the special operations arena where the ATL could be initially fielded.

Previous Research

In order to better understand the situation in the arena of high energy laser (HEL) modeling and simulations, it is necessary to examine the work previously accomplished in the field. Two previous AFIT theses developed the area of laser simulation by examining the way in which HEL weapons were being modeled. Captains Maurice Azar and Michael Cook established a framework for evaluating the ATL in combat simulations which this thesis should attempt to expand upon in the area of target lethality

Research of Captain Maurice Azar

Assessing the Treatment of Airborne Tactical High Energy Lasers in Combat Simulations by Maurice C. Azar (2003) examined the current state of system modeling for the ATL in a scenario set up in the Extended Air Defense Simulation (EADSIM). Captain Azar's scenario utilized a single ATL as a point defense against nine cruise missiles launched from random launch sites within a specified launch area. In order to populate the vulnerability inputs for EADSIM, Captain Azar utilized Tyson's 1st order Brightness equation to determine the power being delivered to the target. From there he worked out a value for radiant flux density and using assumptions about material properties he determined a probability for the delivered energy to destroy the target. He used the populated tables to initialize his scenario and gain insight into the performance of the system. EADSIM uses one table for propagation, which he populated through the use of the brightness equation, and a second table for lethality. He determined the entries for the vulnerablility table through the use of an equation governing the energy required to vaporize a material, and indexed the table by 'survivability percentile'. He concluded that EADSIM version 9.0 was not the most applicable model with which to evaluate the effectiveness of laser weapons, due to the lack of assessment of the variability of the atmosphere, as well as lacking logic for dealing with terrain obscuration of the target after the initiation of the laser engagement. He did however conclude that viable inputs to a campaign level model such as THUNDER could be generated by a mission level model like EADSIM, and included the number of targets killed per engagement and total laser firing time for an engagement. Results from numerous runs would most likely be rolled into a distribution for use by the stochastic campaign model.

Research of Captain Michael Cook

Captain Michael Cook's (2004) thesis, Improving the Estimation of the Military Worth of the Advanced Tactical Laser through Simulation Aggregation used output data from HELEEOS to populate propagation tables for input into EADSIM in order to better examine the evaluation of the military worth of the ATL. This input was used to initialize a number of runs of a scenario in EADSIM designed to measure the effectiveness of the ATL as a military system. For the EADSIM vulnerability tables, Capt Cook used generic levels for radiant flux density (fluence), and indexed the tables using a similar scheme to the one used by Capt Azar. One of the major findings of this work was the observation that HELEEOS and EADSIM (along with other models) exclude non-lethal damage due to the lack of criteria for evaluating 'varying degrees of non-lethal data' (Cook, 04). This partially stemmed from the fact that target vulnerabilities were not well enough developed to evaluate the effect of non-lethal actions taken against them.

Summary

In this chapter we have discussed the modeling hierarchy and identified the level at which the primary model used in this work operates. A description of the Joint Munitions Effectiveness Manual was provided, specifically noting the difficult nature of developing unclassified methods due to the lack of unclassified information about the JMEM. A list of laser issues was laid out, including a history of the DoD development of weaponized lasers, the fundamental problem with laser power falloff over a distance, and an example of the targeting issues associated with distinguishing and designating targets at the ranges involved. A description of the ATL system was provided, and the previous research efforts of Captain Azar and Captain Cook were summarized.

III. Methodology

General Methodology

The purpose of this chapter is to lay out the methodology for conducting this research effort. The specific scenario will be laid out, along with any assumptions which accompany it. A description of HELEEOS, the primary model used in this effort, will be presented, including the specified input being passed to the model, the development of input scripting, and the expected output data. An examination of the Design of Experiments used in this research will be discussed, with an emphasis on factor analysis, ANOVA, and regression techniques.

Scenario

As has been stated previously, the scenario for this research consists of a single ATL system engaging a single ground target. The model for this engagement is patterned after the Concept of Operations (CONOPS) for the UC-130 Spectre Gunship. The target is a stationary generic truck, in the ½ - 1 ton pickup class. The ATL circles the target on a constant radius, similar to the flight path for a gunship engaging ground targets. This allows the ATL to minimize the slewing of the turret over the course of the engagement.

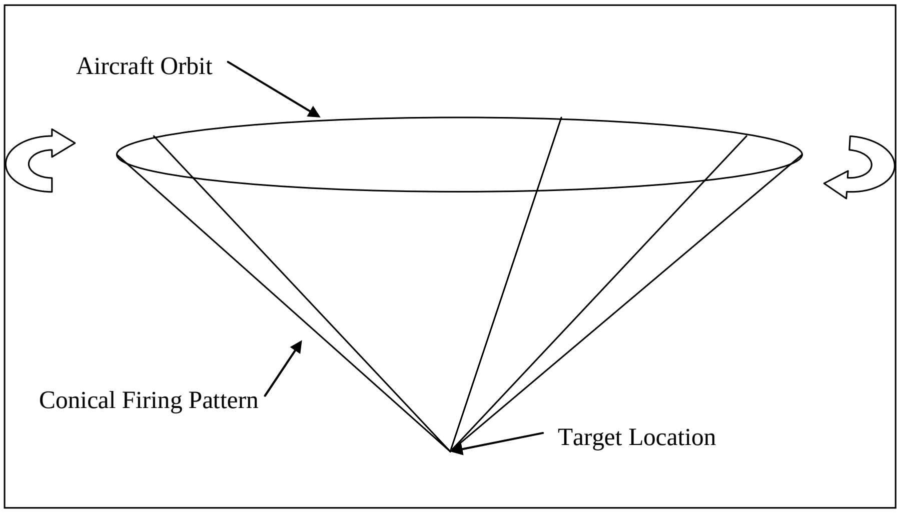

Figure 2: Scenario Geometry

This geometry will also allow the assumption of constant angle of incidence for the duration of the engagement. Given that the ground target is stationary, the slant range is the shortest tested range (2000 meters), and the platform is moving at the maximum tested velocity (129 m/s), the accompanying change in incident angle is 18.3 degrees, with all other engagement geometries resulting in a smaller delta in incident angle.

HELEEOS

Scenario setup will require the specification of a number of inputs for use by the model in the propagation calculations. HELEEOS has a set of inputs which are designated as default and can be loaded by the user via either the Graphical User Interface (GUI) or at the Matlab command line. Some of these values, such as Target Threshold Damage, are used by HELEEOS for p_k calculations, and as such will be irrelevant for this research effort. The model assumes a single aimpoint, and calculates the p_k relative to the user input Target Damage Threshold and Standard Deviation with either a Lognormal or Normal distribution. While this is assumed to be a valid method for determining the probability of kill for a particular aimpoint, one of the purposes of this research is to further investigate options for confirming this method or developing a more applicable method by which to evaluate weapon system performance. It must be noted that HELEEOS assumes perfect tracking (Bartell, 2005), which in reality is impossible. Through the examination of varying target vulnerability parameters such as bucket sizes, and the introduction of jitter, the effect of imperfect tracking can be effectively studied. However, for the purposes of this research, the perfect tracking in HELEEOS will suffice, as what is being developed is not the entire list of factors to be fed to the end table calculations, but the methodology for producing table calculations. An examination of all applicable factors needs to be presented, and any relevant factors not examined for this research need to be noted, for the purposes of completeness.

The following table outlines the initial parameters for HELEEOS. The italicized entries are not varied in this research effort, while the bold entries are those parameters which will need to be either adjusted to match the scenario, or varied for evaluation.

Table 1: HELEEOS Standard Settings

Parameter	Initial Setting
Scenario Type	Static Engagement
Slant Range	**9000m**
Platform Altitude	**3000m**
Target Altitude	0m
Dwell Time	**1 sec**
Platform Velocity Parallel to LOS	0 m/s
Platform Velocity Perpendicular to LOS	**0 m/s**
Target Velocity Parallel to LOS	0 m/s
Target Velocity Perpendicular to LOS	0 m/s
Relative Azimuth	0^0
Susceptible Target Length	**0.05m**
Susceptible Target Width	**0.05m**
Angle of Incidence	90^0
Target Damage Threshold	*50,000,000 J/m*^{2}
Target Damage Threshold STD	*1,000,000 J/m*^{2}
Laser Type	**COIL Laser (High Alt) 1.31525 µm**
Exit Aperture	0.5m
Relative Obscuration	0.3
Power	**50,000 W**
Beam Quality	**1.3**
Wavefront Error	0
Total System RMS Jitter	0
Magazine Depth	**1 sec**
Aerosol Type	**Rural Aerosols**
Atmosphere Type	**U.S. 1976 Standard Atmosphere**
Ground Wind Velocity Perpendicular to LOS	4 m/s
Ground Wind Velocity Parallel to LOS	0 m/s
Turbulence Multiplier	1
Turbulence Profile	HV 5/7

Input Requirements

For the purposes of this research we seek to evaluate the performance of the ATL system over a range of engagement conditions by varying selected inputs to the HELEEOS model described above. The model can be run from a GUI where all of these inputs can be selected as required. This does require user interaction via the keyboard and mouse between model runs, which is not conducive to completing the number of runs required for exhaustive analysis. The model can be run via the Matlab command line, which allows for scripting of repeated runs. The user can specify that the standard inputs are loaded first, and then can adjust any individual input via the command line before initiating a model run.

Factor Levels

In an experimental design, the input parameters which are to be varied are referred to as factors. Some of the input parameters listed in bold in Table 1 are not to be varied, but need to be adjusted from the default setting in order to match the scenario. Table 2 below contains the bold entries from Table 1, with their corresponding corrected values or range of values.

Table 2: HELEEOS Scenario Settings

Parameter	Scenario Settings
Slant Range	2000m
Platform Altitude	2000 - 12000m
Dwell Time	1 - 5 sec
Platform Velocity Perpendicular to LOS	150 - 250 kts
Susceptible Target Length	0.05 - 0.1m
Susceptible Target Width	0.05 - 0.1m
Laser Type	COIL-ATL Simplified High End Power – 40s Run Time
Laser Power	100,000 W
Beam Quality	1.1
Magazine Depth	5 sec
Aerosol Type	Described in Text
Atmosphere Type	Described in Text

For each of the parameters in Table 2 we will now describe the significance of that factor, as well as the reasoning for adjusting or varying it for this scenario. As a general rule, the adjustments are made in order for the input parameters to match the latest projected performance characteristics for the ATL system, while the factors to be varied are those factors which would be loaded into a targeting computer at the time of engagement, and would therefore be directly relevant to required lase time calculations in the field.

Slant Range

For the purposes of this research, the viable slant range over which engagements could take place is 2000 to 12000 meters. The range input vector for slant ranges in meters is as follows:

$$slantRng = [2000\ 3000\ 4000\ 5000\ 6000\ 7000\ 8000\ 9000\ 10000\ 11000\ 12000]$$

This represents the range of geometries from the platform firing straight down from the nominal altitude of 2 kilometers to the platform firing at a ground target ~10 km ground distance away. This researcher believes that this will be one of the driving factors in determining projected engagement lase times, since as has been discussed, beam power falls off with increased distance from the platform to the target. Also, given that the nominal scenario altitude is 2000 meters, this geometry covers the range of engagements from straight down from 2000 meters out to a ground distance of approximately 11,800 meters

Platform Altitude

Platform altitude is set at 2000 meters in order to facilitate the range of engagements required within the Slant Range factor range of values. It is understood that this choice is somewhat arbitrary, but is valid for the scenario as developed. The CONOPS for this scenario differ from previous research efforts in that a ground target is being engaged, while in the work of both Capt. Azar and Capt Cook, the chosen target was a set of multiple targets, resulting in a series of laser engagements. Capt Azar's work used nine cruise missiles in flight, launched from random locations within a specified launch area. For that setup, it would be more appropriate for the ATL to fly at a higher altitude so that engagement ranges could be extended by lessening the target obscuration by the aerosols present in the lower atmosphere. Capt. Azar's EADSIM lookup tables contained data for slant ranges out to 15300 meters while the platform altitude was fixed at 15000 meters. While this geometry provides better visibility for the aircraft to detect and engage airborne targets, it restricts the ground range from the platform to ~3000 meters. Capt. Cook's scenario involved engaging ground targets which were simulated by zero velocity cruise missiles placed at zero altitude. He also utilized longer slant ranges (out to 15000m), but also varied the altitude between 1000, 4500, and 8000 meters. While it may be possible for the laser to deliver lethal fluence at these ranges, it was noted at the DEPS conference that it may not be possible for the targeting optics to effectively discern and designate targets at these ranges. The chosen scenario altitude allows the platform the option of engaging targets out toward the limit of the targeting optics (DEPS Conference, 2005). Additionally, the 2000 meter engagement altitude is above the 1525 foot boundary layer, below which most of the atmospheric aerosols are contained (Bartell, 2005) Without further evidence to the contrary, this altitude and slant range pairing will allow engagements within the performance envelope of the ATL and may allow insight into viable maximum engagement distance parameters.

Dwell Time

While lase time will be the ‘knob’ by which desired p_{eff} will be ‘dialed’ within the analysis portion of this work, a reference set by which this factor can be evaluated must be varied within the experimental design. The vector for lase time in seconds is as follows:

$$dwellTime = [1 \ \ 1.5 \ \ 2 \ \ 2.5 \ \ 3 \ \ 3.5 \ \ 4 \ \ 4.5 \ \ 5]$$

The projected laser magazine for the ATL is currently 100 seconds of lase time (Boeing, 2005), and the scenario defined 1-5 second lase time will allow for between 20 and 100 engagements per sortie. It may be determined that longer lase times will be required for extended distances near the upper edge of the slant ranges defined. This may be a factor which will determine the correct engagement ranges over which the laser would be used in normal operating conditions.

Platform Velocity

In order to determine the correct CONOPS for any airborne platform, consideration must be given to airspeed. The vector for platform velocities, converted from knots to meters per second is as follows:

$$platformVel = [77 \ \ 90 \ \ 103 \ \ 116 \ \ 129]$$

The C-130 is capable of flight in excess of 250 knots, but for the purposes of this scenario, we will limit the airspeed to 250 knots. HELEEOS uses velocity measured in m/s, which for the stated scenario range of 150 to 250 knots translates to 77 to 129 m/s. As was stated before, this should not violate the assumption of constant incident angle for the laser at the target, as the maximum change in incident angle is obtained at the shortest engagement slant range and is only 18.7^0 given the aircraft is traveling at the maximum velocity of 129 m/s for a full 5 second engagement.

Susceptible Length/Width (Bucket Size)

The Susceptible Length and Width parameters are used to describe the ‘bucket’ into which energy can be deposited on the target in order to cause damage. The vector for the bucket size parameter in meters is as follows:

$$spotSize = [.01\ \ .02\ \ .03\ \ .04\ \ .05\ \ .06]$$

When the input is made, the Length factor and Width factor are varied symmetrically (Length = Width), and the resultant levels are simply each of the six listed levels squared. This factor is varied to simulate the variance in target vulnerability by aimpoint or desired effect. It may be determined that for a particular aimpoint it is less important that the spot be maintained in a small area. As an example, in order to light the vehicle interior on fire, it may not be as important to maintain a fixed spot as it is to burn a hole in the hood or fuel tank. This may allow the former as a viable aimpoint at a greater range than the later two, as spot point maintenance becomes more difficult with increasing range. An interesting note from the screening runs is that for bucket sizes above .0025 m^2, (.05m * .05m), the power in the bucket did not vary, meaning that the entire beam spot was contained in the bucket. Given that result, the initial levels from .05m to .1m were changed to the levels listed above. The .06m level was retained in order to attempt to replicate the observation from the screening runs and to possibly account for beam spread at longer engagement ranges than were used in the screening runs.

Laser Type

HELEEOS supports a number of laser types and wavelengths, each with their appropriate atmospheric absorption and scattering characteristics. For this research, we will implement the High Powered ATL COIL Laser defined in the model's laser types. This is a COIL laser with a wavelength of 1.317µm. Within the model this laser type is denoted as laser type seven.

Laser Power

The current projected Initial Operational Capability (IOC) for the ATL power output is 100kW (Boeing, 2005). Previous research has used either 50kW or 50kW and 100kW laser output levels. Since we are attempting to replicate the currently projected system as it will be fielded, this research uses a fixed laser output power of 100kW.

Beam Quality

One of the optical characteristics of a laser beam is Beam Quality. A 'perfect' Gaussian beam is given a value of 1, with beam qualities typically falling in the 1.1 – 1.5 range (as seen by the author). This rating is a measure of the focusability of the laser and governs the distribution of the laser spot across the surface of the target. The current projected ATL system lists a beam quality of 1.1 (Boeing, 2005).

Magazine Depth

For the currently projected system IOC, the magazine depth is listed as 100 seconds of lase time. Though lase times for this scenario are limited to 5 seconds, and there is no tracking of total lase time between scenario engagements, the magazine depth must be at least 5 seconds. This is because each run consists of a single engagement where previous work has looked at multiple engagements within a single model run. In order to match the system as closely as possible, the magazine will be set to 100 seconds.

Aerosol Type

HELEEOS contains data for a number of different aerosol type profiles. Aerosols are the fine matter particulates in the air which are more prevalent in the lower atmosphere. As was noted above, these particulates are for the most part contained in the atmosphere below 1525 feet. These particulates impede the propagation of a laser beam by absorbing energy and diffracting the beam. These will be adjusted within the scenario to match the last factor, Geographic Area, in order to replicate the specified atmospheric environment.

Geographic Area

Within this scenario, geographic area is varied over 5 regions: Average Weather, Mid Latitude, Coastal, Rugged Terrain, and Chaparral. The current Boeing system assumptions lists these five environments as the atmospheric conditions of interest to the development of ATL modeling. Within the HELEEOS model, these regions will be represented by the 1976 Average atmosphere, Mid Latitude atmosphere, and the Expert Atmospheric data for Langley, Nellis, and Davis-Monthan, respectively. All calculations are made at a 50^{th} percentile value for relative humidity, and are based on the summer data numbers (where summer and winter settings exist).

Input Script Development

In order to adjust the input parameters to the specified levels and to vary the experimental factors, a Matlab script with a nested looping structure has been developed. Capt Cook used a script with two loops in order to vary platform altitude and slant range over his scenario values in order to develop a propagation table for input into EADSIM. This script was modified in order to perform further variations and gain additional insight into the laser propagation over a larger range of input values, to adjust parameters to this scenario, and to calculate additional outputs. Appendix A contains the script along with the relevant code comments.

Output Data

Within the input script, the output for each design point is fed into a data array, and after all model runs have been completed, the array is written out to a comma separated text file for import in to Microsoft Excel or other software package for data analysis. The outputs initially gathered are as follows: Peak Irradiance (W/m^2), Average Irradiance (W/m^2), Fluence based on Peak Irradiance (J/m^2), Fluence based on Average Irradiance(J/m^2), and Power in the Bucket (W). The fluence numbers are calculated based on the reported numbers for irradiance because in the course of performing screening runs, it was discovered that the fluence number being output by the model was a number of orders of magnitude larger than should have been expected, given the geometries and lase times. The fluence numbers are calculated using the following equation:

$$Fluence = Irradiance \times Lase\ Time$$

Energy in the Bucket is also listed, and is calculated as follows:

Energy in the Bucket = Power in the Bucket x Lase Time

It is hoped that additional insight can be gained by examining this larger number of outputs, in an attempt to find a measure by which the laser can be accurately and effectively evaluated. A number of preliminary screening runs are being performed in order to confirm that the input variation of the factors works as intended, and to see if there are any issues which may arise from large data output. One initial run consisted of 11881 design points, and took 1.65 hours to complete computation running on an Athlon64 2800+ system with 1 gigabyte of memory. From this initial effort we can see that scalability of the input factors in number and number of levels is limited only by our ability to capture and analyze the data. For the sake of simplicity and portability, we will limit the number of design points to the number of data row elements which we can capture in a spreadsheet tool for manipulation. Current Microsoft Excel 2003 worksheets are limited to 65,533 data rows, thus an additional factor with 5 levels could be explored without exceeding our imposed limit. Given that the processing time required to complete these runs is directly proportional to the number of runs being performed, we should expect a computing time of approximately 9 hours if the full data output capability is utilized.

Design of Experiments

This effort will use a full factorial experiment design, where every factor is varied across every available level of every other factor. This is generally the least computationally efficient method, but considering the length of any given run is on the order of seconds, full enumeration of all factor levels outweighs the minimal time required to do so. Additionally, a number of replications for each treatment (or set of factor levels) is generally run. The output from HELEEOS is deterministic, and therefore additional replications for each treatment gain nothing in terms of statistical significance. Also, because the model is deterministic, as was mentioned in Chapter 2, the model runs do not need to be randomized in their order because the model output is deterministic and is independent of time or run order.

The initial expected end-product for this research will consist of a tool to be used for development of JMEM type data. The tool will be based on a linear regression model which will be constructed to predict the output power of the laser system given a set of inputs and will be adapted to 'tune' the output to the required level by adjusting one of the input variables.

ANOVA stands for Analysis of Variance, which is another method of studying the relation between a response variable and the associated input or explanatory variables. ANOVA models do not require any statistical assumptions about the nature of the explanatory variables, nor do they require those variables to be strictly quantitative. Given that the geographic factor for laser output power is a qualitative variable, it follows that an ANOVA model would be developed in order to aid in the construction of the regression model. Should two levels of the geographic factor be shown to be statistically different, it would follow that they should use different regression equations to model the power output. On the other hand, should they be shown to not be statistically different, and then we would be justified in using the same regression model for both of the factor levels.

Factor Analysis

In order to better understand the influence of each of the input variables on the power output given by the model, a number of multivariate analysis techniques will be applied to the data. Multivariate analysis is the application of methods that deal with large numbers of measurements made on each object simultaneously (Dillon, 1). Objects in this case are individual design points, and the measurements are the individual factor levels for each output observation. These techniques move away from univariate and bivariate analyses which concentrate only on individual or pairwise analysis of variables and looks at the covariance between three or more variables simultaneously. While this may prove overkill given the number of input factors identified for this study, it is important to initially explore all options for analysis which seem relevant to the area of analysis.

Vulnerability Assessment

The vulnerability assessment portion of this work is where the largest change from previous efforts occurs. While the previous work used vulnerability en-route to some other higher level output factor as a MOE, this research is restricted to an exploration of the vulnerability assessment itself. The intention is to fill out and solidify the concepts and methodology for developing and presenting this vulnerability data in order to create a product which a current JMEM user would find familiar and easy to use. Using empirical test data instead of theoretical values for required radiant flux density, as well as evaluating multiple aimpoints, will aid in more accurately evaluating the vulnerability of targets to interdiction by a laser system.

Materials Assessment

The data for required radiant flux densities was obtained from AFRL/DE by specifying particular thicknesses of steel, painted steel, and rubber which correspond to the aimpoint configuration for the designated target for this scenario. The data returned lists the required flux density in joules per square centimeter required to burn a hole in the specified material. The following is a list of the specified materials, thicknesses and the energy required to realize the desired effect.

Table 3: Vulnerability Data

Material	Thickness	Energy Required to Melt	Irradiance	Critical Irradiance
Primed and Painted Steel	0.080”	2500 J/cm^2	500 W/cm^2	50 W/cm^2
Primed and Painted Steel	2 Layers, 0.080” (Second layer bare)	5000 J/cm^2	500 W/cm^2	50 W/cm^2
Primed and Painted Steel	0.160”	5000 J/cm^2	500 W/cm^2	50 W/cm^2
Primed and Painted Steel	2 Layers, 0.160” (Second layer bare)	9900 J/cm^2	500 W/cm^2	50 W/cm^2

Table 3 notes that for any given target point, there is a Critical Irradiance level, which represents the threshold above which the laser output power at the target must remain in order to accumulate the required energy to melt the target material. This level is the level of input energy below which the target will just ‘get hot’ instead of accumulating enough energy to begin the process of melting. For reference, the .080” thickness represents 14-gauge steel, and the .160” thickness is 8-gauge steel, both common thicknesses used in vehicle construction. The body panels on a light truck would be represented by the 14-gauge sample, while a heavy duty truck may incorporate the thicker 8-gauge sample in some components. Though the scenario calls for a single ground target, since the target has been previously defined as a pickup truck in the ½ - 1 ton class, these samples encompass the range of viable target aimpoint materials for this class of target.

At this point it makes sense to review the process of imparting a desired effect to a target via energy deposited by a laser beam. The laser beam imparts energy to the surface until, assuming the energy is being added at a wattage level above the critical irradiance threshold described above, a number of effects may take place. The material can transition to liquid form (melt), vaporize, or ignite and burn or char. For the purposes of this research, we will be concentrating on the melting of the material, and will 'hand wave' the energy lost to the vaporization and burning phenomena by the adjustment of the vulnerability threshold. Additionally, for the data obtained, these represent the worst case scenario for each of the target configurations. What is meant by worst case is that this configuration assumes the worst case for any of the given inputs for target characteristics. Specifically, for the two layer samples, there may be portions of the target surface where the layers are separated by some distance (assumed up to and including 1cm). This configuration is common in vehicle construction, such as in the support rib sections underneath the hood of our fictional truck. In this separated configuration, the second bare layer would absorb the energy from the laser better than in the non-separated case, and would therefore require less energy to melt through both layers while separated (as opposed to non-separated). The painted surface for the samples was assumed to be white paint, which has the lowest absorption rate for any paint color. Any darker color would absorb at a faster rate and again require less energy to be deposited in order to attain melt-through (Thompson, 2005). Thus, this data set represents the 'hardest' target within this class by assuming white paint color, and worst specific particular aimpoint characteristics by assuming there is a second metal layer non-separated from the surface layer.

To compensate for the variation in target construction material, the damage threshold for this work will be ten percent higher than the figures listed in Table 3. It is understood that this adjustment is rather arbitrary, but is relevant as a correction factor for the purposes of real world planning calculation replication. The critical irradiance threshold will be maintained at the same level, as it is assumed there may just be up to ten percent of extra material or material energy absorption capability which would simply require the additional energy deposited at the original threshold for accomplishment of melt-through.

Concept of Operations Considerations

As was mentioned above, the basic concept of operations for the ATL has been assumed to be similar to that of the current UC-130 Spectre gunship. The expected model output should contain sufficient data to perform an initial survey of viable engagement parameters for the operation of the ATL. By evaluating the relation of various input factors to the power output of the laser at the target, a clearer picture of which factors may be ignored and which factors may warrant further investigation. As an example, it may be found that platform velocity has such a small influence on power output within a given range of other inputs as to recommend that the CONOPS for flight speed be set according to fuel consumption rather than laser output. On the other hand, the exact opposite may be true, and flight speed should be set so as to utilize some characteristic of a particular speed. All of the viable alternatives warrant initial investigation Care should taken that previous research given similar data is examined and contrasted, while at the same time gaining additional insight from the addition of design points.

Summary

The methodology chapter provided an explanation of the general research plan for the remainder of this work. The scenario was laid out, including the background justification for engagement geometry. The primary model, HELEEOS, was described, and a detailed explanation of all pertinent input factors was provided. The input scripting process was outlined, and initially gathered output responses were defined. The design of experiments used in this research was reviewed, concluding that the full factorial experiment used, though not computationally efficient, is the most applicable for exploration of factor analysis. Finally, a description of the vulnerability portion comprising the greatest advance of this research over previous work was discussed, with special attention paid to the examination of target vulnerability assessment.

IV. Analysis and Results

Chapter Overview

This chapter contains the core of the analysis work done and will build from initial data verification analysis to ANOVA and factor influence analysis. It will conclude with an investigation of viable weapon system engagement profiles and presentation of system performance in a tabular format. Initial data verification will investigate the model output and will attempt to confirm that physical phenomena which are expected based on the scenario setup are correctly represented in the data. The ANOVA will attempt to determine which of the factors are the most significant to power output. Finally, we will present a regression model to predict peak power output, which can then be used to evaluate inputs against the vulnerability thresholds for a given aimpoint.

Results of Simulation Scenarios

The final experimental design contained an additional two atmospheric types, giving a total of seven atmospheres, nine lase times, five values for platform velocity, six bucket sizes, and eleven slant ranges, for a total of 20,790 design points. For each of these points, output was recorded for peak irradiance, average irradiance, fluence based on peak irradiance, fluence based on average irradiance, and power in the bucket. After the data was recorded, a unit conversion was performed. HELEEOS outputs for irradiance and fluence are in W/m^2 and J/m^2 respectively, and the vulnerability data obtained from AFRL/DE is in W/cm^2 and J/cm^2, so the first four outputs were multiplied by a factor of $1/10{,}000$ to convert from $1/m^2$ to $1/cm^2$. This allows direct comparison between the unit converted data and the data acquired for the purposes of vulnerability assessment.

For each of the inputs, there is an expected relationship with the output power which is based on the physics involved with the scenario. For example, we expect both the peak and average intensity to increase as slant range decreases, as the laser is passing through less of the atmosphere. These relationships can be seen by plotting the output data against the inputs to see if the expected pattern appears. We will investigate all the inputs against the output data in their input order: slant range, lase time, platform velocity, atmosphere type, and bucket size.

For the slant range, as stated above, the researcher expects the power at the target to fall off as distance to the target increases.

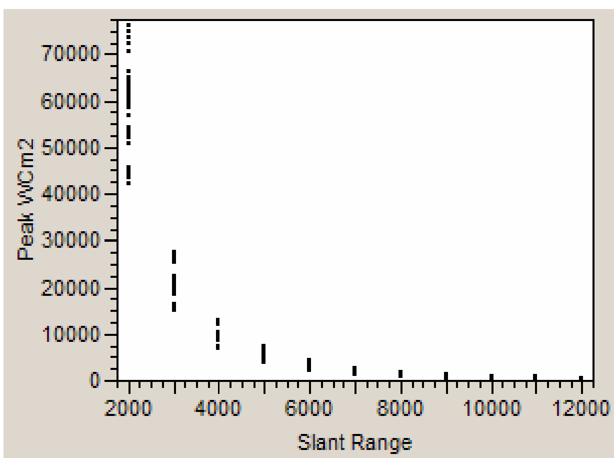

Figure 3: Peak Irradiance vs. Slant Range

Figure 3 shows the unit converted peak irradiance values plotted against slant range. We can see that the power at the target does indeed fall off with increased slant range, but there is some stratification of the data at each range, meaning there is another factor involved, and we would initially identify atmosphere as a possible culprit.

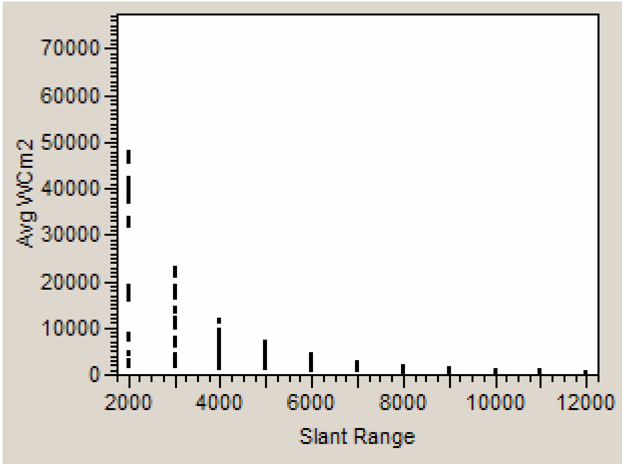

Figure 4: Average Irradiance vs. Slant Range

Figure 4 shows the unit converted average irradiance values plotted against slant range. As expected, power does fall off with increased range, but the variance in the data suggests that there is something in addition to our initial guess of atmospheric stratification as a reason for variance, as the values for even the closest range fall off almost to zero, and there appear to be a number of widely distributed groups within that one range. On initial investigation, it appears that the bucket size is the factor involved here, and it did not appear in the peak values above because bucket size affects the average irradiance, but not the peak. This will be explained and expanded on in the section on bucket size later in this section.

For the lase time factor, we expect energy deposited to increase as lase time increases. This should be apparent in the plots of both peak and average fluence over lase time.

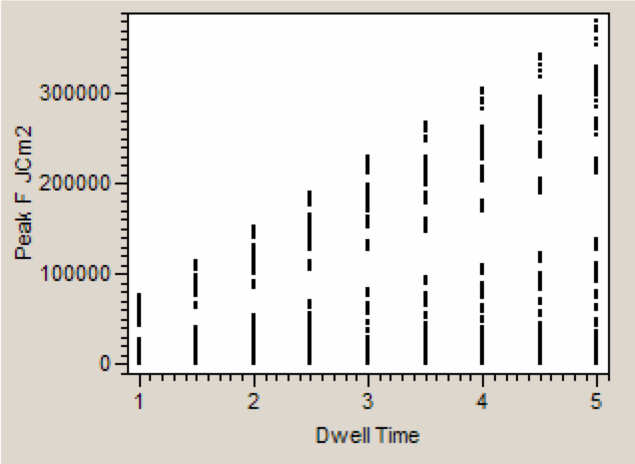

Figure 5: Peak Fluence vs. Dwell Time

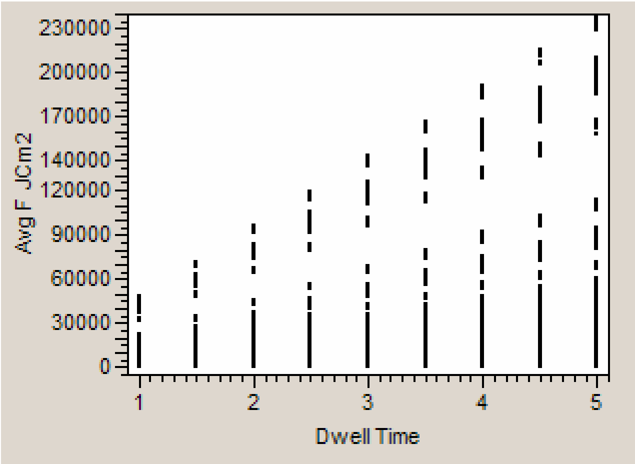

Figure 6: Average Fluence vs. Dwell Time

Figures 5 and 6 show the linear increase of fluence at the target with increased dwell time. There again seems to be a stratification based on atmosphere, slant range, and bucket size. The reason all three of these factors are identified as interactions is as follows: since irradiance falls off with increasing range, the fluence at each dwell time value will contain the values for all slant ranges. Also, since there are different levels of irradiance for the varying atmospheres, this will also cause multiple irradiances for each dwell time level. Finally, as bucket size increases, the average irradiance decreases, and again causes multiple fluence levels for each dwell time level.

Next, as platform velocity increases, we expect an increase in the peak irradiance at the target, and a subsequent increase in fluence and PIB, due to the mitigation of the effects of thermal blooming caused by the laser more rapidly slewing though the atmosphere.

Figure 7: Peak Irradiance vs. Platform Velocity

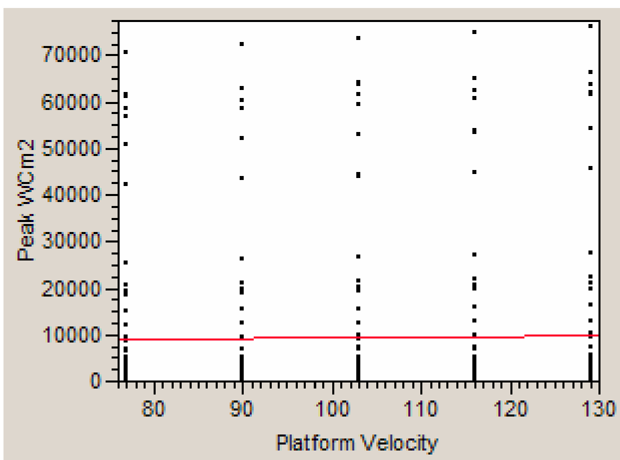

Figure 7 shows that although there is a difference in the output performance of the laser, it is very slight across all the levels tested. From the JMP output for this plot, the linear fit for peak irradiance is as follows:

$$Peak\ \left(W/Cm^2\right) = 7966.33 + 14.03\ Platform\ Velocity$$

This means that for the increase from 77 to 129 meters per second, the average for peak irradiance increased 729.56 W/cm^2, or 9.16%. Since the maximum efficient cruising speed of a C-130 is 177 m/s, and this speed is well above the values tested for this work, we will from this point forward use only the output values corresponding to the maximum tested platform velocity of 129 m/s.

For the atmospheric factor, we made no assumption about the difference which each of the atmospheres would have on the output data, but expected to see some variance, based on the physical properties of the atmosphere at each of the chosen geographic locations. If you will recall from Chapter III, the seven atmospheric types are: the 1976 Average data, Mid-Latitude data, and the HELEEOS ExPERT data for Langley, Nellis, Davis-Monthan, Hail (Saudi Arabia), and the Gibraltar Civilian/Military airfields. After performing a one-way ANOVA for this factor using JMP, it was discovered that three of the levels were not statistically significantly different.

Table 4: Atmospheric Means Analysis

Level		Peak Irradiance
Gibraltar	A	11953.125
Langley	B	9727.992
Hail	B	9652.636
Davis Monthan	B	9652.636
Nellis	C	9195.436
1976 Standard	D	8682.046
Mid Latitude	E	7018.191
Levels not connected by the same letter are significantly different		

Table 4 lists the mean peak irradiance for each of the atmospheric factor levels, and the center column shows to which mean group the level belongs. JMP determines this statistical significance using the Tukey-Kramer HSD test. Given that the Gibraltar data and the Langley data are both from coastal regions, while the Hail data and Nellis data were both considered chaparral, it is apparent that the initial assumption about these outputs being similar was incorrect. It has instead been shown that the Langley, Davis-Monthan, and Hail outputs are statistically the same, and all other atmospheric levels are different. This means that when a regression is developed to attempt to predict laser output, the inclusion of atmosphere as a predictor should only contain five statistically differing estimates for regression coefficients.

Finally, we expect to see a decrease in average fluence for a given slant range as the bucket size increases. This is because as the bucket size increases, there is more area over which we are averaging the beam strength, while at the same time we are capturing more of entire beam spot. However, we should also see a limit to this pattern, because once the entire beam has been captured, we are then averaging the energy being deposited over a larger and larger area. Power in the Bucket should be the output measure by which this phenomenon should be most readily discernable, because unlike the average, the PIB number does not fall off after the entire beam spot has been captured, as it is an integration of the energy deposited over the area of the spot, rather than of the bucket. Thus, as the bucket increases, PIB should also increase, but only until the entire spot has been captured, at which point the PIB output should remain constant. From the screening runs we noted that for all the bucket sizes investigated, the PIB number remained almost constant, meaning the buckets were too large for the increasing PIB with bucket size phenomena to be observed, as we were already capturing the entire spot. For the screening runs, the bucket sizes ranged from $(5cm)^2$ to $(10cm)^2$, and since we noted the lack of change in PIB, the bucket sizes for the production runs were changed to $(1cm)^2$-$(6cm)^2$. With this information in hand, an analysis of PIB over slant range was performed for a single atmospheric level and platform velocity level.

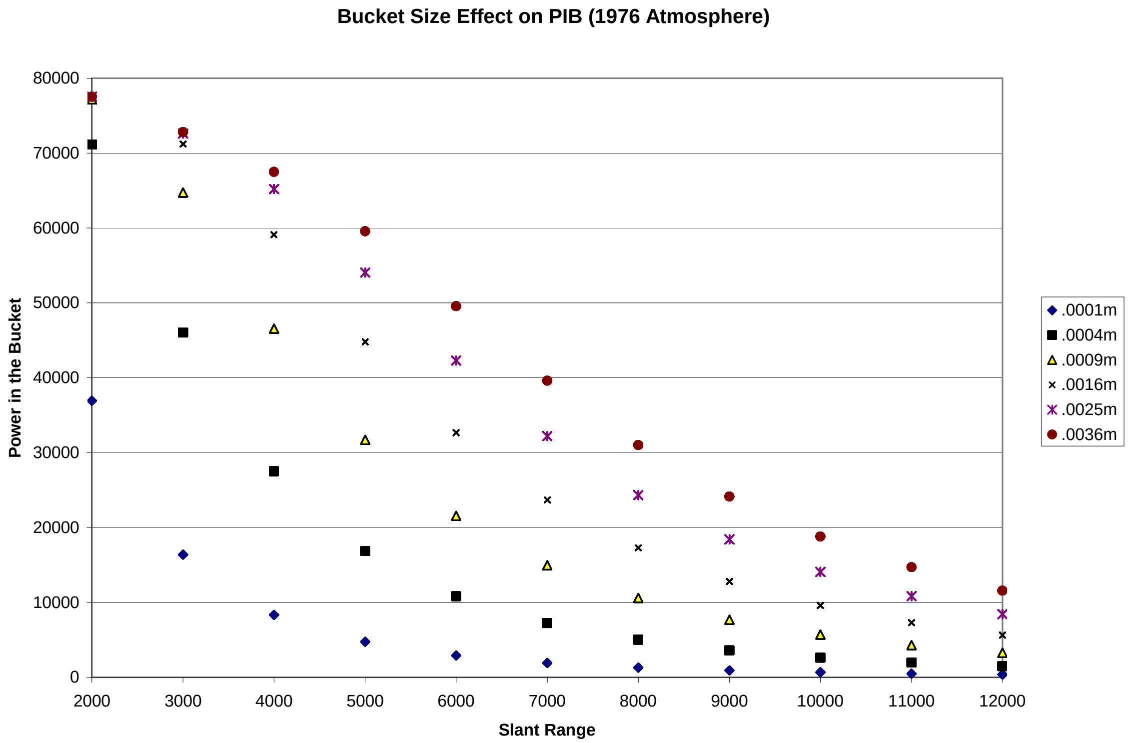

Figure 8: Bucket Size Analysis

Figure 8 shows that as the bucket size increases, the corresponding PIB also increases, but is limited by the size of the spot at a given range. It can be seen that at the minimum range of 2000 meters, the entire spot energy has been captured in the $9cm^2$ bucket, and as the range becomes larger and the spot size increases, the full energy is not captured until the larger bucket sizes. Since during the screening runs it was observed that the PIB output did not increase significantly between bucket sizes out to 4000 meters, it was assumed that the entire spot was being captured for these larger bucket sizes, and the decision was made to change to the set of smaller buckets. After performing the analysis on the production data, there is still some question as to the proper bucket size to use for targeting purposes. After discovering the pattern displayed in Figure 8 above, the same analysis was run on the screening data for the same atmosphere and platform velocity, and a similar pattern was discovered.

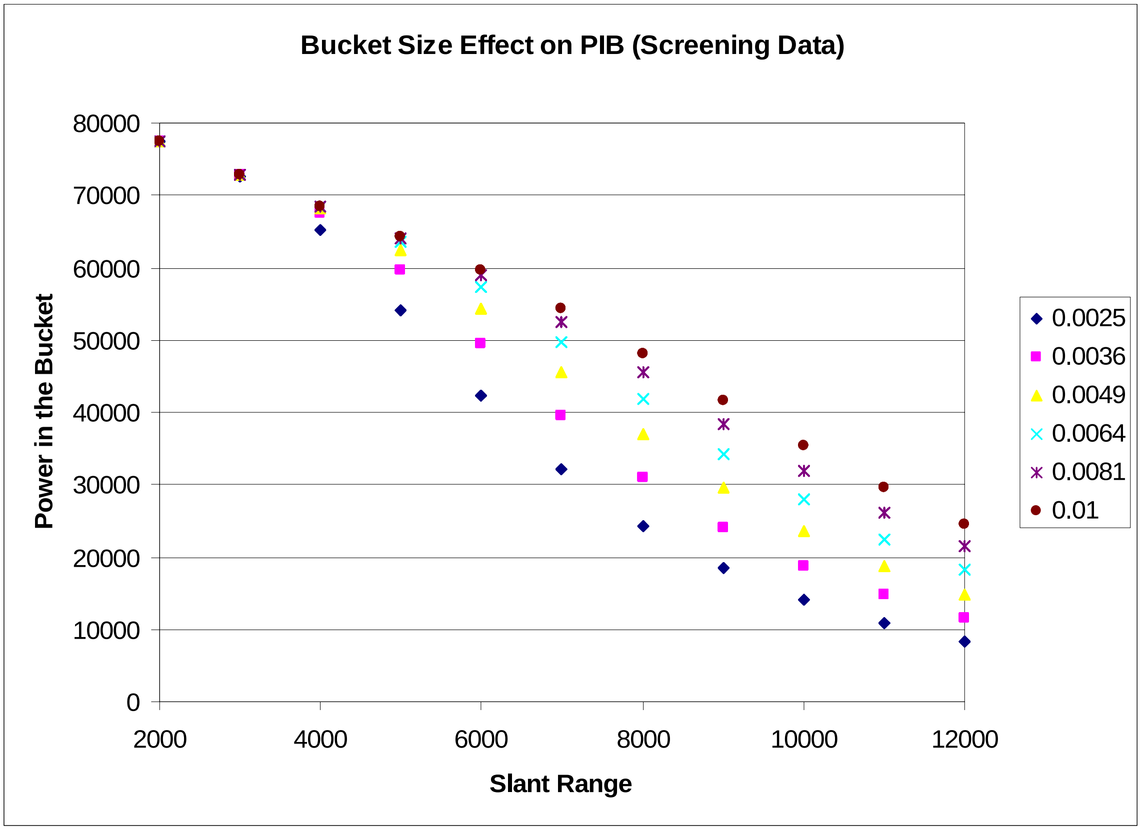

Figure 9: Screening Run Bucket Size Analysis

We can see that as the slant range increases, there is a significant difference in the amount of energy being deposited depending on the bucket size. While this is indeed an interesting result, though the PIB output increases with bucket size, the average irradiance continues to fall off for the larger buckets, and is especially distorted at close ranges. For example, at a 2000 meter slant range with a .01m^2 bucket, the average irradiance is 775 W/cm^2 and the peak is 50900 W/cm^2, while with a .0036m^2 bucket, the average irradiance is 2150 W/cm^2 with the same peak. Thus it is apparent that we need to choose a spot size large enough to capture the majority of the beam profile, but not so much that the peak value is 'washed out' over the large bucket area. This suggests picking a value toward the smaller end of the screen run bucket sizes, but on the upper side of the production runs. We therefore will restrict further investigation to the 36 cm2 bucket size, both to capture the entire spot size, and to limit the area over which we are attempting to cause the desired effect.

Predictive Model

After the initial screening of the data, in order to formulate a predictive model for the output, linear regression techniques were applied to the data. The number of design points was reduced by limiting the bucket size to the 36cm^2 level and the platform velocity to the 129m/s level. The original set of factor levels was [7 9 5 6 11] resulting in a total of 20,790 design points. The reduced set of factor levels is [7 9 1 1 11], giving a total of 693 design points.

In order to most accurately predict the number of seconds of dwell time required to exceed the threshold criteria for each aimpoint in Table 3, we have determined that it would be most applicable to consider the average irradiance across our chosen bucket size. According to the Intermediate Value Theorem from calculus, we know that for any continuous function on a closed interval [*a*,*b*] where *c* is between *f(a)* and *f(b)*, there is some x^* on [a,b] such that $f(x^*)=c$ (Mendelson, 114). Additionally, we know that if c is the mean value for the function over [a,b], $f(x)$ decreases monotonically over [a,b], and that $f(b) < f(x^*) = c$, then it is necessary that $f(a)>f(x^*)=c$. We know that the irradiance falls off with distance from the center of the laser spot, and does so monotonically. The short explanation of all the previous math is to explain that if we are concerned with satisfying a energy threshold within a given aimpoint, and calculate the amount of time required to reach that threshold based on the average irradiance across the spot, then if we satisfy that threshold on average, we have more than exceeded the threshold at the peak irradiance at the center of the spot and have therefore most definetly satisfied the threshold somewhere within the aimpoint bucket.

From the nature of the physics involved, we can see that except in cases of extreme thermal blooming, the irradiance at the spot is independent of dwell time, and we therefore can not include that factor as a regressor. This leaves the atmospheric type and slant range as our inputs for a regression model. Since we have already determined that not all of the scenario atmospheres are statistically different, we should expect that the betas for the regression for each of these levels should be very similar or identical. We will however initially use all of the levels as predictors in order to confirm this result before combining atmospheres. Additionally, it makes sense to go ahead and predict the unit converted average irradiance, as linear regression will produce identically comparable models when predicting any output and any linear transformation of that input. Since the unit conversion involves only a linear transformation (dividing by 10,000), the transformation will not interfere with the predictive capability of the model.

In order to be sure of the correct prediction based on atmospheric level, six binary dummy variables were coded, with atmosphere 1 representing the baseline, and each of the other atmospheric levels represented by a binary variable. This ensures that the betas output by JMP® are coded correctly. Using the minimum mean sqare error method of linear regression, the model for predicted average irradiance using all levels of the atmospheric factor and slant range as regressors, JMP® outputs the following for the model:

Summary of Fit	
RSquare	0.981741
RSquare Adj	0.981675
Root Mean Square Error	4.962949
Mean of Response	1060.247
Observations (or Sum Wgts)	6.93

Analysis of Variance				
Source	DF	Sum of Squares	Mean Square	F Ratio
Model	7	2538801.3	362686	14724.85
Error	1917	47217.4	25	Prob > F
C. Total	1924	2586018.6		0

Parameter Estimates				
Term	Estimate	Std Error	t Ratio	Prob>|t|
Intercept	2509.6273	6.503493	385.89	0
Atm 2	-192.6364	7.054029	-27.31	<.0001
Atm 3	-335.1818	7.054029	-47.52	0
Atm 4	-249.0909	7.054029	-35.31	<.0001
Atm 5	-132.9091	7.054029	-18.84	<.0001
Atm 6	-132.9091	7.054029	-18.84	<.0001
Atm 7	64.454545	7.054029	9.14	<.0001
Slant Range	-0.18709	0.000596	-313.8	0

Figure 10: Linear Regression Model Including All Atmospheres

From the parameter estimates in Figure 10 we can see that according to the regression, atmospheric levels five and six are identical since they have the exact same beta value. This was expected, as this was evidenced in the Tukey-Kramer HSD test performed in Table 4 above. However, from this test we expected that atmospheric level three should also be associtiated with levels five and six. It is apparent in the reduced data set that there is some difference in the means across the atmospheric factor levels. In order to confirm this, the Tukey-Kramer HSD was re-run on the reduced data set, and is displayed in Table 5.

Table 5: Tukey-Kramer HSD for Reduced Data

Level					Average Irradiance
Gibraltar	A				1264.4545
1976 Standard	A				1200
Davis Monthan		B			1067.0909
Hail		B			1067.0909
Mid Latitude		B	C		1007.3636
Nellis			C		950.9091
Langley				D	864.8182
Levels not connected by same letter are significantly different					

This re-evaluation of the data in the reduced set indicates that for some reason, the third atmospheric level now has the lowest mean, and that only levels five and six are strictly related. Level two straddles the five/six group and level four, and should thus have a beta value between the values for these level groups. A review of the information in Figure 10 shows that this is indeed the case. Since we only have data for one replication, this test will only detect larger differences in the means. Using only three replications of the data, the means separate into six distinct levels. The Davis-Monthan and Hail data remains identical, and we therefore can combine the atmospheric levels for these two atmospheres. This is accomplished by coding a new binary dummy variable which contains a 1 in the rows where the atmosphere equals either Davis-Monthan or Hail, and zero otherwise. This variable is then added to the model, while the variables for atmospheric levels five and six are removed. This substitution will result in a reduction in the number of degrees of freedom used in the model, without any reduction in the predictive power of the model as represented by the value for R^2 not being reduced. Additionally, during recoding and further investigation it was observed that the slant range squared is also a significant factor for prediction and was added to the model. Using this new coding scheme, the model was re-run and the following results were observed:

Summary of Fit	
RSquare	0.989548
RSquare Adj	0.98951
Root Mean Square Error	3.754927
Mean of Response	1060.247
Observations (or Sum Wgts)	6.93

Analysis of Variance				
Source	DF	Sum of Squares	Mean Square	F Ratio
Model	7	2558989.9	365570	25927.9
Error	1917	27028.7	14	Prob > F
C. Total	1924	2586018.6		0

Parameter Estimates				
Term	**Estimate**	**Std Error**	**t Ratio**	**Prob>|t|**
Intercept	2448.513	5.178768	472.8	0
Atm 7	64.45455	5.337022	12.08	<.0001
Atm 2	-192.6364	5.337022	-36.09	<.0001
Atm 3	-335.1818	5.337022	-62.8	0
Atm 4	-249.0909	5.337022	-46.67	0
Atm 5/6	-132.9091	4.621996	-28.76	<.0001
Slant Range	-0.18709	0.000451	-414.8	0
(Slant Range-7000)^2	6.1E-06	1.62E-07	37.84	<.0001

Figure 11: Regression Results with Consolidated Atmospheres for Reduced Data

Figure 11 shows that all levels are significant because all of the Prob>|t| values are much less than the commonly accepted cutoff of .05. This regression gives the following equation for estimating average irradiance (W/cm^2)output:

Equation 1:

$$
\begin{aligned}
Irradiance\ (W/cm^2) = {} & 2448.5134 + \left(-192.6364 \times Atm\,2\right) + \left(-335.1818 \times Atm\,3\right) \\
& + \left(-249.0909 \times Atm\,4\right) + \left(-132.9091 \times Atm\,5/6\right) \\
& + \left(64.4545 \times Atm\,7\right) + \left(-0.1871 \times Slant\ Range\right) \\
& + \left[(Slant\ Range - 7000)^2 \times 0.00000611\right]
\end{aligned}
$$

Where the Atm variables represent the atmospheric type, and are equal to 1 if the atmosphere is of that type, and are zero otherwise.

As an example, we will evaluate this equation for a sample design point. Given the input factor levels given in Table 6, we will perform the regression and determine the approximate value for the average irradiance from HELEEOS given in the last column of the table.

Table 6: Example Regression Calculation Data

Slant	Dwell	P Vel	Atmos	Spot	Irradiance
2000	1	129	1	0.0036	2154

Substituting these values into Equation 1 gives:

Equation 2: Example Regression Calculation

$$
\begin{aligned}
Irradiance\ (W/cm^2) = {} & 2448.5134 + \left(-192.6364 \times 0\right) + \left(-335.1818 \times 0\right) \\
& + \left(-249.0909 \times 0\right) + \left(-132.9091 \times 0\right) \\
& + \left(64.4545 \times 0\right) + \left(-0.1871 \times 2000\right) \\
& + \left[(2000 - 7000)^2 \times 0.00000611\right] \\
= {} & 2227.12
\end{aligned}
$$

This gives an error of -77.12 or -3.39% for this data point. Using this percentage based error, the error remains relatively small until the slant ranges reach the 10,000m range, where the extreme error appears to be limited to the Langley atmosphere. Plotting the percent error against slant range, the following pattern emerges:

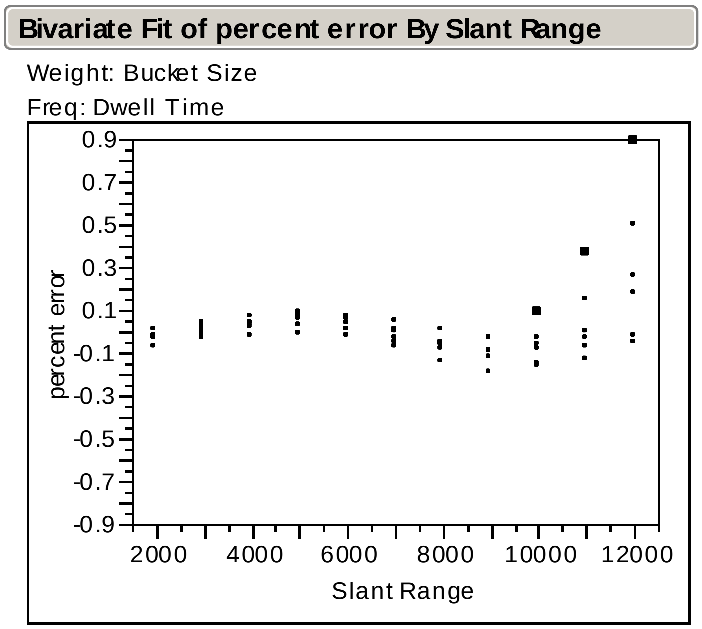

Figure 12: Percent Error by Slant Range

We can see that the percent error versus slant range plot in Figure 12 exhibits a sinusoidal pattern, and by examining the Durbin-Watson autocorrelation score, we can see that there is definetly some issue with correlation between the responses. What is interesting is that the highlighted points in Figure 12 are all from the Langley atmosphere, and the three points directly below those highlighted points are from the Nellis atmosphere. The highest point is for the Langley atmosphere where actual average irradiance is 179 W/cm^2 and the predicted average irradiance is 21.04 W/cm^2. This indicates that there is some interaction over slant range which was not apparent when the lower platform velocities and smaller bucket sizes were still included. One possible explanation is that the effects of thermal blooming are mitigated more in the closer ranges for the Langley atmosphere due to the nature of a coastal/maritime atmosphere, and there is a stronger interaction between these factors as range increases. Adding all of the interactions between slant range and the coded variables scales the percent error closer to zero, but does not at all mitigate the sinusoidal pattern exhibited in Figure 12.

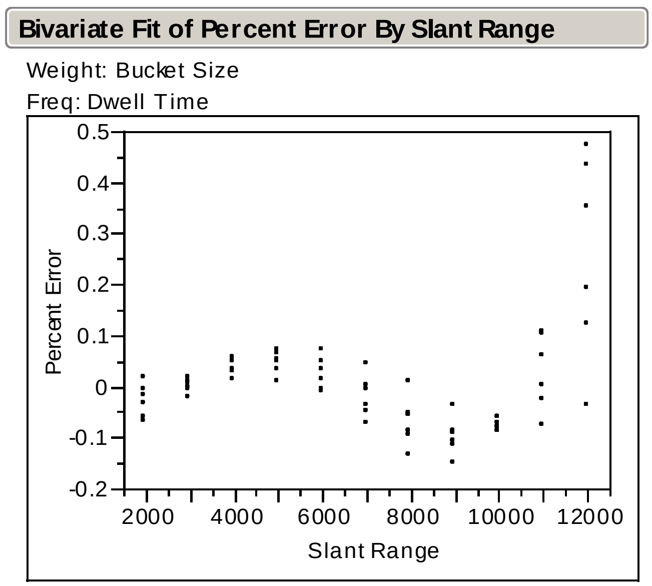

Figure 13: Error by Slant Range Including Interactions

Based on p-values, the Mid-latitude atmosphere interaction with slant range is not significant, and based on the betas for the other interactions, we are well enough off without any of these additional interactions included. The sinusoidal pattern in Figure 12 continues in Figure 13, simply scaled toward zero across the slant ranges. This points to an area for further study, as it seems that some unknown underlying factor is influencing the output as slant range increases. However, the model is not grossly under-estimating the output until the extreme ranges of the scenario, where based on the level of irradiance it would not be possible to effect damage within the imposed five-second per shot time limit. We will therefore press forward using the model as established in Equation 1 and will now begin the process of producing predictive output for a JMEM like data table.

Vulnerability Assessment

Now that the predictive model has been established, we will begin the process of evaluating the laser against the chosen target evaluation criteria. If the reader will recall, Table 3 listed the vulnerability data provided by AFRL/DE; however it was decided that this data would be scaled upward by ten percent in order to account for manufacturing inconsistencies and general conservativeness.

Table 7: Scaled Vulnerability Data

Aimpoint	Material	Thickness	Energy Required to Melt	Critical Irradiance
1	Primed and Painted Steel	.080"	2750 J/cm^2	50 W/cm^2
2	Primed and Painted Steel	2 Layers, .080" (Second layer bare)	5500 J/cm^2	50 W/cm^2
3	Primed and Painted Steel	.160"	5500 J/cm^2	50 W/cm^2
4	Primed and Painted Steel	2 Layers, .160" (Second layer bare)	10890 J/cm^2	50 W/cm^2

Note that Table 7 does not contain the column for irradiance from Table 3. This column has been excluded as this value will be determined by the output from Equation 1, and will be used to determine the number of seconds of dwell time required in order to cause the desired effect. Additionally, it is important to note that though the output from

Equation 1 does predict values for irradiance below the critical irradiance threshold, the actual data never drops below this level. In either case, these data points reside at the longest slant ranges and due to the level of irradiance both produced and predicted, the energy required for melt-through would not be reached due to dwell time limit as opposed to not meeting the critical irradiance requirement.

With these pieces of information in hand, we can now proceed to develop vulnerability tables for our target, with entries for each of the aimpoints described in Table 7. Because the linear regression equation is valid for points within the range of the data for which it was originally developed, we can confidently interpolate slant ranges between those entered in the original design. The entire range of resulting tables are listed in Appendix C, but for the purposes of discussion we will examine a table for Atmosphere 5/6, which the reader will recall are Davis-Monthan and Hail, Saudi Arabia. The reduction of Equation 1 for this atmosphere is as follows:

$$\begin{aligned} Avg\,(W/cm^2) = {} & 2448.5134 + (-192.6364 \times (0)) + (-335.1818 \times (0)) \\ & + (-249.0909 \times (0)) + (-132.9091 \times (1)) \\ & + (64.4545 \times (0)) + (-.1881 \times Slant\ \ Range) \\ & + \left[(Slant\ \ Range - 7000)^2 \times 0.00000611\right] \end{aligned}$$

From this equation we can use the slant range column of the table to predict irradiance, and then can determine the number of seconds required to melt through the chosen aimpoint. Number of seconds required for melt-through is generated from the following function:

$$Seconds\ \mathrm{Re}quired = \begin{cases} \dfrac{Threshold}{\mathrm{Pr}edicted\ Irradiance} & if\ \dfrac{Threshold}{\mathrm{Pr}edicted\ Irradiance} \leq 100 \\ N/A & Otherwise \end{cases}$$

Table 8: Predicted Time to Melt-Through for Atmosphere 1

Atm	Slant Range	Irradiance	Aim 1	Aim 2	Aim 3	Aim 4
1	2000	2225.06	1.2	2.5	2.5	4.9
1	2250	2163.15	1.3	2.5	2.5	5.0
1	2500	2101.99	1.3	2.6	2.6	5.2
1	2750	2041.60	1.3	2.7	2.7	5.3
1	3000	1981.97	1.4	2.8	2.8	5.5
1	3250	1923.11	1.4	2.9	2.9	5.7
1	3500	1865.01	1.5	2.9	2.9	5.8
1	3750	1807.68	1.5	3.0	3.0	6.0
1	4000	1751.10	1.6	3.1	3.1	6.2
1	4250	1695.30	1.6	3.2	3.2	6.4
1	4500	1640.25	1.7	3.4	3.4	6.6
1	4750	1585.97	1.7	3.5	3.5	6.9
1	5000	1532.45	1.8	3.6	3.6	7.1
1	5250	1479.70	1.9	3.7	3.7	7.4
1	5500	1427.71	1.9	3.9	3.9	7.6
1	5750	1376.49	2.0	4.0	4.0	7.9
1	6000	1326.02	2.1	4.1	4.1	8.2
1	6250	1276.33	2.2	4.3	4.3	8.5
1	6500	1227.39	2.2	4.5	4.5	8.9
1	6750	1179.22	2.3	4.7	4.7	9.2
1	7000	1131.81	2.4	4.9	4.9	9.6
1	7250	1085.17	2.5	5.1	5.1	10.0
1	7500	1039.29	2.6	5.3	5.3	10.5
1	7750	994.18	2.8	5.5	5.5	11.0
1	8000	949.82	2.9	5.8	5.8	11.5
1	8250	906.24	3.0	6.1	6.1	12.0
1	8500	863.41	3.2	6.4	6.4	12.6
1	8750	821.35	3.3	6.7	6.7	13.3
1	9000	780.05	3.5	7.1	7.1	14.0
1	9250	739.52	3.7	7.4	7.4	14.7
1	9500	699.75	3.9	7.9	7.9	15.6
1	9750	660.75	4.2	8.3	8.3	16.5
1	10000	622.50	4.4	8.8	8.8	17.5
1	10250	585.03	4.7	9.4	9.4	18.6
1	10500	548.31	5.0	10.0	10.0	19.9
1	10750	512.36	5.4	10.7	10.7	21.3
1	11000	477.17	5.8	11.5	11.5	22.8
1	11250	442.75	6.2	12.4	12.4	24.6
1	11500	409.09	6.7	13.4	13.4	26.6
1	11750	376.20	7.3	14.6	14.6	28.9
1	12000	344.06	8.0	16.0	16.0	31.7

From Table 8 we can see a fall-off in the ranges at which the ATL is capable of inflicting the required amount of damage as the threshold moves up across the selected aimpoints. This limit is of course arbitrary, and is based on our prescribed CONOPS limit of five seconds for any particular shot. The tables listed in Appendix C are built such that this arbitrary restriction is removed, and only the critical irradiance criteria is checked. Thus the maximum time for the listings in those tables is the hard limit of 100 seconds of lase time as dictated by the current projected ATL system capabilities.

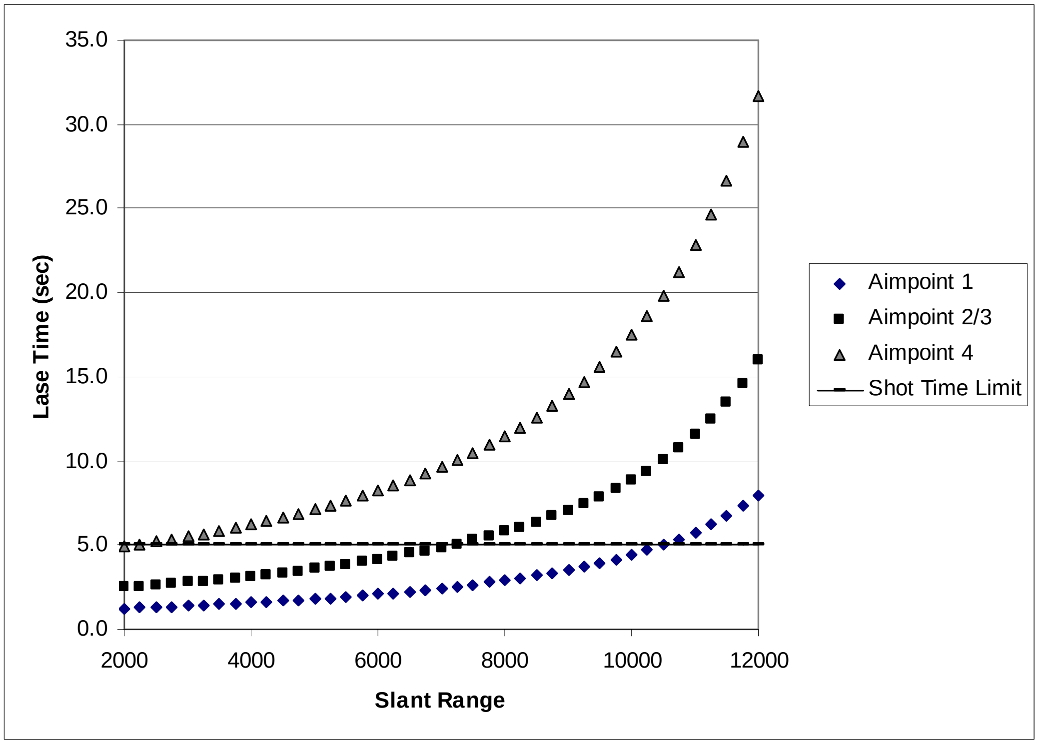

Figure 14: Required Lase Time Over Slant Range, by Aimpoint, for Atmosphere 1

Figure 14 shows the increasing lase time required for melt-through, with the original five second time limit depicted as a horizontal line across all the ranges. Note that for the 'hardest' aimpoint, the lase time limit cuts all but the very first point. This indicates that this aimpoint would not be a viable selection for the given CONOPS. However, for this atmosphere, irradiance never falls below the critical irradiance value, so for a high-value target there is enough irradiance at longer ranges to effect melt-through, given clearance to exceed the shot time limit. This also assumes the target will remain in the same relative geometry with the ATL over the entire course of the engagement. This assumption may cause issues with thermal blooming, as the model was only run out to times of five seconds, but this is unknown to the researcher at this time. This pattern exhibited in Figure 14 exists across all atmosphere types. However in the third and fourth atmospheric types, there are a number of points for which there is not enough irradiance to meet the critical irradiance threshold or not enough time within the hard limit of 100 seconds to cause melt-through.

Summary

This chapter has reviewed the results of the simulation and examined the outputs to validate the data based on the researcher's understanding of the physics involved with the problem. A number of the outputs were examined after being plotted vs. various inputs, and insight was gained into the 'shape' of the data. The bucket size input was examined, and after examination was limited to the 36 cm^2 level. Similarly, the platform velocity was also examined, and based on the flight characteristics of the C-130, was limited to the 129 m/s level. A regression equation was then developed for use in population of vulnerability tables. After re-statement of the adjusted vulnerability characteristics for each of the aimpoints, the tables were developed and analyzed.

V. Conclusions and Recommendations

Chapter Overview

This chapter summarizes the results of this research effort, and will attempt to draw conclusions from the scenario output. Deviations from the original research plan will be listed and explained. It will expand on and explain the significance of the results and will make recommendations for action based on the results as presented. Though Chapter 4 contains the bulk of the analysis of the data, this chapter will highlight areas where further exploration is warranted. It will then conclude with suggestions for future research in the field.

Evolution of Research Plan

There were a number of areas in which the research evolved from the original and intermediate plans, one due to time constraints, one to researcher inexperience with programming in Matlab, and one to a lack of available data. First, multivariate factor analysis was listed in Chapter 3 as one of the techniques which would be used to investigate the influence of any underlying factors on the inputs which would in turn influence the outputs. It first appeared as this technique would be unnecessary, as all of the apparent physical phenomena were being explained through exploration of the inputs themselves without regard for any possible underlying factors. Only after the development and examination of the linear regression model for output prediction did any indication that additional influences were at work appear. The outputs were considered good enough to press on, as the anomalies were out at the furthest ranges examined, where the reduction in overall output power caused the laser to run out of magazine before causing the required level of damage. Further multivariate analysis may be justified in order to find the source of this behavior.

Second, two additional atmospheric types were computed through Matlab user miscoding on the part of the researcher. The original vector for the atmospheric type was coded as [‘na’ ‘na’ 147 190 71]. When a call is made to return the third, fourth, and fifth elements of this vector, [n], [a], and [147] are returned. Since the evaluation uses the numeric value for the characters, the returned values became [110], [97], and [147]. The input listing for geographic sites lists Hail, Saudi Arabia as entry 110, and the Gibraltar Civ/Mil Air Station as entry 97. It was determined that this data should not be wasted, given the computational expense of having calculated the outputs for these atmospheres, and they were therefore recoded as atmospheres 6 and 7, respectively. The script was then corrected and re-run in order to confirm that the coding error was as discovered, at the expense of having to re-calculate the outputs for atmosphere 3. When the corrected outputs for atmosphere 3 matched the previously recorded values for atmosphere ‘5’, the coding error was considered correctly diagnosed, and the data output for atmospheres 6 and 7 were appended to the corrected run output.

Finally, data was not able to be obtained for the generic ‘tire’ aimpoint for reasons undisclosed to the researcher. The original request for information contained a ¼” thickness rubber target, which would have been used to represent a sidewall shot on a tire for the truck. This data would have to have been restricted on the slant range factor, because in most cases the tires are not targetable in the geometry of the closest slant ranges, as the angle of attack prohibits line of sight to the aimpoint. This aimpoint data was requested for the specific purpose of simulating a particular aimpoint for which the resulting p_{eff} could be directly linked to the delay or disable categories of the JMEM data picture. The researcher understands that AFRL/DE is time and manpower restricted, and is grateful that the four other aimpoint data requests were filled expediently. It is our opinion that this data may be available at the classified level, but was not able to be obtained in unclassified form within the time restriction imposed by the researcher's graduation date. This lack of vulnerability data will be brought up again in the areas for further research section below.

Conclusions of Research

From the vulnerability tables produced in Chapter 4, it is apparent that given the projected capabilities of the ATL system, there are limits to the applicability of those capabilities based on range to target, atmospheric profile, and target vulnerability characteristics. It has been shown in previous research that there are a number of other factors which can influence the irradiance reaching the target, such as jitter, atmospheric relative humidity, and others. The purpose of this research was not to create a complete picture of all the factors which influence irradiance at the target, but was to develop a methodology for creating JMEM type outputs for the ATL weapon system. Given that goal, we have created a straightforward lookup table based on atmosphere and slant range which returns the number of 'rounds' of lase time (in seconds) which are required to effect the required damage at a number of different aimpoints. This framework is extensible by later considering other output influencing factors in the development of the regression equations, or by evaluating the predicted output against additional aimpoint vulnerabilities. Additionally, the output from a model such as HEELEOS could be used to predict irradiance for a more accurate estimate of actual lase times required. The advantage of the regression approach is that given the input levels, the required output can be calculated by hand if necessary. While this may not necessarily be an advantage for an individual calculation, any calculation that can be done manually can also be done en-masse in a spreadsheet, which is where the real advantage lies.

The vulnerability tables produced for Appendix C show the increase in required lase time without regard for the artificially constructed per-shot time limit of five seconds established as a part of this scenario. These tables allow a planner to evaluate the cost in terms of magazine percentage utilized to achieve the effect of melt-through at the aimpoints given for the scenario's generic truck target. These tables represent an assumed one hundred percent p_{eff} for either delaying or disabling the target. This assignment to the delay and disable categories is arbitrary, as the researcher is not a JMEM user by trade, and the researcher would defer to the judgment of a more experienced end user for p_{eff} classification.

The listing of the vulnerability threshold surpassing point as seconds of lase time is not arbitrary, and was done so that the most logical comparison between a laser weapon and a similarly targeted conventional weapon could be performed. Because the capacity of the laser magazine is listed in seconds of lase time, it seems most appropriate to list the required 'number of munitions' to effect damage as lase time in seconds as well. This allows the JMEM end user to make an evaluation as to the worth of 1 second of lase time in a given delivery profile against the worth of a conventional weapon delivered similarly.

Significance of Research

For any developmental weapon system, it is necessary to explore initial capabilities and to compare those capabilities with currently available weapon systems. It is especially important in the case of laser weapons, as this comparison must be done thoughtfully, and with regard for the inherent differences between laser and conventional weapons. This research has presented a coherent view of the issues involved with predicting and producing damage with laser weapons, and has laid the groundwork for extension by the laser vulnerability community. The propagation and target vulnerability profiles utilized are directly applicable to questions about the initial capability of the ATL weapon system. Finally, the output tables produced can be used not only for initial baseline comparisons, but are applicable to the development of the CONOPS for the ATL, as they can be used in tradeoff analysis for mission effectiveness based on maximum allowable per-shot lase time.

Recommendations for Action

This document and the associated data is being forwarded to members of the JMEM/FX lethality working group in hopes that it will have sufficiently moved the discussion about this topic forward to justify expansion of this work vice replication. The JMEM/FX Chairperson has requested that the output data, analysis, and conclusions be forwarded to their office for review and possible expansion.

Recommendations for Future Research

- Given the nature of laser effects research being done at the classified level, it is recommended that this research be passed on for evaluation given 'better' vulnerability data.

- The researcher was unable to obtain data for the generic tire aimpoint. This additional work would be directly applicable to evaluation for delaying or disabling this specific target type, as well as other wheeled vehicles.

- Additional HELEEOS exploration of the lase time and bucket size input factors would help clarify whether extended lase times for this scenario would cause issues with the thermal blooming phenomena, and whether increased bucket size would be more applicable at extended ranges, respectively.

- Tradeoff analysis for CONOPS consideration should be performed in order to determine the correct cutoff for per-shot lase time, in order to maximize military utility given the currently projected magazine limit of 100 seconds.

Summary

This work presented the problem of the necessity for development of JMEM type data for the ATL weapon system. A review of the available unclassified literature was performed, exploring the issues associated with the problem. Some of these issues include modeling of laser propagation, previous assumptions about target vulnerabilities, and the inherent differences between laser and conventional weapons. A methodology was laid out, using the output from a validated physics based model to produce a linear regression equation for predicting average irradiance, and from that predicted value, generating a lase time required to meet various vulnerability thresholds. The output from the HELEEOS model was analyzed to confirm that the data appeared as expected, and to determine which of the input factors were significant, or could be limited to specific levels for use in the development of the regression model. The regression model was constructed, and an analysis of the predictive capabilities of the model was performed. It was discovered that there was some unseen factor underlying the output, as there was a distinct sinusoidal pattern in the residual data. This discrepancy was determined to be small enough, and located far enough toward the extreme ranges of the system for the developed predictive model to be applicable for the predominant range of projected engagements. The model was then used to develop predicted outputs for a set of scenario points, and those predictions were used to populate vulnerability tables. Through the use of actual AFRL/DE laser test data instead of theoretical energies required to cause the effect, the researcher attempted to more accurately predict the required lase time to cause the specified effects. Deviations from the original research plan were then listed, and were followed by the conclusions reached by the researcher. Finally, recommendations were made for future research in the field, and specifically for application to this problem.

Appendix A: HELEEOS Script

```
function HELEEOS_Comparison;
%Declare the structure data as a global
global data
% DATA SETUP *********************************************

tic
heleeosSetDefaults;

%Define and load variables to be varied
slantRng = [2000 3000 4000 5000 6000 7000 8000 9000 10000 11000 12000]
dwellTime = [1 1.5 2 2.5 3 3.5 4 4.5 5];
platformVel = [77 90 103 116 129];
spotSize = [.01 .02 .03 .04 .05 .06];
geography = [1 2 3 4 5 6 7];
geoloc = [1 2 8 8 8 8 8];
% geomap locations: [n/a n/a Langley Nellis Davis-Monthan]
geomap = [1 1 147 190 71 110 97];

data.In.laserType = 7;
data.In.platformAltitude = 2000;
data.In.targetAltitude = 10;
data.In.wavefrontError = .000000263
data.In.susceptibleRegionLen = .05;
data.In.susceptibleRegionWid = .05;
data.In.laserPower = 100000;
data.In.windVelPerpen = 4; data.In.windVelParallel = 0;
data.In.groundWindVel = sqrt(data.In.windVelPerpen.^2+data.In.windVelParallel.^2);
data.In.platformVelParal = 77;
data.In.platformVelPerpe = 0;
data.In.targetVelParal = 0;
data.In.targetVelPerpe = 0;
data.In.sigmaJitter = 0;
data.In.sigmaTotalJitter = 0;
data.In.turbulanceMultiplier = .9;
data.In.atmospheretype = 1;

%  HELEEOS EXECUTION CYCLE ******************************
p = 1;
for i = 1:length(slantRng);
for j = 1:length(dwellTime);
for k = 1:length(platformVel);
for l = 1:length(geoloc);
for m = 1:length(spotSize);

%Used for loop verification testing
% for i = 1:2;
% for j = 1:2;
% for k = 1:2;
% for l = 1:2;
% for m = 1:2;

   data.In.slantRange = slantRng(i);
```

```
    data.In.engageDwell = dwellTime(j);
    data.In.platformVelParal = platformVel(k);
    data.In.atmosphereType = geoloc(l);
    if l > 2
        data.Map.stationID = geomap(l);
        data.In.atmospherePercentileType = 5;
    end
    data.In.susceptibleRegionLen = spotSize(m);
    data.In.susceptibleRegionWid = spotSize(m);
    heleeosCalc;
    OutData(p,1) = slantRng(i);
    OutData(p,2) = dwellTime(j);
    OutData(p,3) = platformVel(k);
    OutData(p,4) = geography(l);
    OutData(p,5) = spotSize(m) ^ 2;
%   Commented out due to error in data.Out.fluence computation within
%   HELEEOS
%   OutData(p,6) = real(data.Out.fluence);
%   Note: due to the discovery of this error by the researcher, the output has since been
%   corrected
    OutData(p,7) = max(data.Out.irrTotalAtmosUserSpotSize);
    OutData(p,8) = heleeosCalcAvgIrr(data.Out.irrTotalAtmos3DUserSpotSize);
    OutData(p,9) = dwellTime(j) * max(data.Out.irrTotalAtmosUserSpotSize);
    OutData(p,10) = dwellTime(j) * heleeosCalcAvgIrr(data.Out.irrTotalAtmos3DUserSpotSize);
    OutData(p,11) = data.Out.irrTotalAtmosUserSpotSizePIB;

    p = p + 1;

end
end
end
end
end

%Write output data structure to comma delimited file
toc
runtime = toc
csvwrite('output.csv',OutData);
return
```

Appendix B: Reduced Output Data for Regression

Slant	Dwell	Atm	Bucket	Peak	Average	Peak F	Average F	PIB	Avg W/Cm2
2000	1	1	0.0036	544000000	21500000	544000000	21500000	77525	2150
2000	1.5	1	0.0036	544000000	21500000	816000000	32300000	77525	2150
2000	2	1	0.0036	544000000	21500000	1090000000	43100000	77525	2150
2000	2.5	1	0.0036	544000000	21500000	1360000000	53800000	77525	2150
2000	3	1	0.0036	544000000	21500000	1630000000	64600000	77525	2150
2000	3.5	1	0.0036	544000000	21500000	1900000000	75400000	77525	2150
2000	4	1	0.0036	544000000	21500000	2180000000	86100000	77525	2150
2000	4.5	1	0.0036	544000000	21500000	2450000000	96900000	77525	2150
2000	5	1	0.0036	544000000	21500000	2720000000	108000000	77525	2150
3000	1	1	0.0036	200000000	20200000	200000000	20200000	72808	2020
3000	1.5	1	0.0036	200000000	20200000	300000000	30300000	72808	2020
3000	2	1	0.0036	200000000	20200000	400000000	40400000	72808	2020
3000	2.5	1	0.0036	200000000	20200000	500000000	50600000	72808	2020
3000	3	1	0.0036	200000000	20200000	600000000	60700000	72808	2020
3000	3.5	1	0.0036	200000000	20200000	700000000	70800000	72808	2020
3000	4	1	0.0036	200000000	20200000	800000000	80900000	72808	2020
3000	4.5	1	0.0036	200000000	20200000	899000000	91000000	72808	2020
3000	5	1	0.0036	200000000	20200000	999000000	101000000	72808	2020
4000	1	1	0.0036	95600000	18800000	95600000	18800000	67729	1880
4000	1.5	1	0.0036	95600000	18800000	143000000	28200000	67729	1880
4000	2	1	0.0036	95600000	18800000	191000000	37600000	67729	1880
4000	2.5	1	0.0036	95600000	18800000	239000000	47000000	67729	1880
4000	3	1	0.0036	95600000	18800000	287000000	56400000	67729	1880
4000	3.5	1	0.0036	95600000	18800000	335000000	65800000	67729	1880
4000	4	1	0.0036	95600000	18800000	383000000	75300000	67729	1880
4000	4.5	1	0.0036	95600000	18800000	430000000	84700000	67729	1880
4000	5	1	0.0036	95600000	18800000	478000000	94100000	67729	1880
5000	1	1	0.0036	52900000	16800000	52900000	16800000	60341	1680
5000	1.5	1	0.0036	52900000	16800000	79400000	25100000	60341	1680
5000	2	1	0.0036	52900000	16800000	106000000	33500000	60341	1680
5000	2.5	1	0.0036	52900000	16800000	132000000	41900000	60341	1680
5000	3	1	0.0036	52900000	16800000	159000000	50300000	60341	1680
5000	3.5	1	0.0036	52900000	16800000	185000000	58700000	60341	1680
5000	4	1	0.0036	52900000	16800000	212000000	67000000	60341	1680
5000	4.5	1	0.0036	52900000	16800000	238000000	75400000	60341	1680
5000	5	1	0.0036	52900000	16800000	265000000	83800000	60341	1680
6000	1	1	0.0036	32200000	14100000	32200000	14100000	50789	1410
6000	1.5	1	0.0036	32200000	14100000	48200000	21200000	50789	1410
6000	2	1	0.0036	32200000	14100000	64300000	28200000	50789	1410
6000	2.5	1	0.0036	32200000	14100000	80400000	35300000	50789	1410
6000	3	1	0.0036	32200000	14100000	96500000	42300000	50789	1410
6000	3.5	1	0.0036	32200000	14100000	113000000	49400000	50789	1410
6000	4	1	0.0036	32200000	14100000	129000000	56400000	50789	1410
6000	4.5	1	0.0036	32200000	14100000	145000000	63500000	50789	1410
6000	5	1	0.0036	32200000	14100000	161000000	70500000	50789	1410
7000	1	1	0.0036	20800000	11400000	20800000	11400000	41006	1140
7000	1.5	1	0.0036	20800000	11400000	31200000	17100000	41006	1140
7000	2	1	0.0036	20800000	11400000	41700000	22800000	41006	1140
7000	2.5	1	0.0036	20800000	11400000	52100000	28500000	41006	1140

Slant	Dwell	Atm	Bucket	Peak	Average	Peak F	Average F	PIB	Avg W/Cm2
7000	3	1	0.0036	20800000	11400000	62500000	34200000	41006	1140
7000	3.5	1	0.0036	20800000	11400000	72900000	39900000	41006	1140
7000	4	1	0.0036	20800000	11400000	83300000	45600000	41006	1140
7000	4.5	1	0.0036	20800000	11400000	93700000	51300000	41006	1140
7000	5	1	0.0036	20800000	11400000	104000000	57000000	41006	1140
8000	1	1	0.0036	14100000	8990000	14100000	8990000	32367	899
8000	1.5	1	0.0036	14100000	8990000	21200000	13500000	32367	899
8000	2	1	0.0036	14100000	8990000	28300000	18000000	32367	899
8000	2.5	1	0.0036	14100000	8990000	35400000	22500000	32367	899
8000	3	1	0.0036	14100000	8990000	42400000	27000000	32367	899
8000	3.5	1	0.0036	14100000	8990000	49500000	31500000	32367	899
8000	4	1	0.0036	14100000	8990000	56600000	36000000	32367	899
8000	4.5	1	0.0036	14100000	8990000	63700000	40500000	32367	899
8000	5	1	0.0036	14100000	8990000	70700000	45000000	32367	899
9000	1	1	0.0036	9960000	7030000	9960000	7030000	25313	703
9000	1.5	1	0.0036	9960000	7030000	14900000	10500000	25313	703
9000	2	1	0.0036	9960000	7030000	19900000	14100000	25313	703
9000	2.5	1	0.0036	9960000	7030000	24900000	17600000	25313	703
9000	3	1	0.0036	9960000	7030000	29900000	21100000	25313	703
9000	3.5	1	0.0036	9960000	7030000	34900000	24600000	25313	703
9000	4	1	0.0036	9960000	7030000	39800000	28100000	25313	703
9000	4.5	1	0.0036	9960000	7030000	44800000	31600000	25313	703
9000	5	1	0.0036	9960000	7030000	49800000	35200000	25313	703
10000	1	1	0.0036	7220000	5490000	7220000	5490000	19772	549
10000	1.5	1	0.0036	7220000	5490000	10800000	8240000	19772	549
10000	2	1	0.0036	7220000	5490000	14400000	11000000	19772	549
10000	2.5	1	0.0036	7220000	5490000	18000000	13700000	19772	549
10000	3	1	0.0036	7220000	5490000	21700000	16500000	19772	549
10000	3.5	1	0.0036	7220000	5490000	25300000	19200000	19772	549
10000	4	1	0.0036	7220000	5490000	28900000	22000000	19772	549
10000	4.5	1	0.0036	7220000	5490000	32500000	24700000	19772	549
10000	5	1	0.0036	7220000	5490000	36100000	27500000	19772	549
11000	1	1	0.0036	5360000	4300000	5360000	4300000	15493	430
11000	1.5	1	0.0036	5360000	4300000	8030000	6460000	15493	430
11000	2	1	0.0036	5360000	4300000	10700000	8610000	15493	430
11000	2.5	1	0.0036	5360000	4300000	13400000	10800000	15493	430
11000	3	1	0.0036	5360000	4300000	16100000	12900000	15493	430
11000	3.5	1	0.0036	5360000	4300000	18700000	15100000	15493	430
11000	4	1	0.0036	5360000	4300000	21400000	17200000	15493	430
11000	4.5	1	0.0036	5360000	4300000	24100000	19400000	15493	430
11000	5	1	0.0036	5360000	4300000	26800000	21500000	15493	430
12000	1	1	0.0036	4050000	3390000	4050000	3390000	12206	339
12000	1.5	1	0.0036	4050000	3390000	6070000	5090000	12206	339
12000	2	1	0.0036	4050000	3390000	8100000	6780000	12206	339
12000	2.5	1	0.0036	4050000	3390000	10100000	8480000	12206	339
12000	3	1	0.0036	4050000	3390000	12100000	10200000	12206	339
12000	3.5	1	0.0036	4050000	3390000	14200000	11900000	12206	339
12000	4	1	0.0036	4050000	3390000	16200000	13600000	12206	339
12000	4.5	1	0.0036	4050000	3390000	18200000	15300000	12206	339
12000	5	1	0.0036	4050000	3390000	20200000	17000000	12206	339

Slant	Dwell	Atm	Bucket	Peak	Average	Peak F	Average F	PIB	Avg W/Cm2
2000	1	2	0.0036	456000000	20400000	456000000	20400000	73439	2040
2000	1.5	2	0.0036	456000000	20400000	684000000	30600000	73439	2040
2000	2	2	0.0036	456000000	20400000	912000000	40800000	73439	2040
2000	2.5	2	0.0036	456000000	20400000	1140000000	51000000	73439	2040
2000	3	2	0.0036	456000000	20400000	1370000000	61200000	73439	2040
2000	3.5	2	0.0036	456000000	20400000	1600000000	71400000	73439	2040
2000	4	2	0.0036	456000000	20400000	1820000000	81600000	73439	2040
2000	4.5	2	0.0036	456000000	20400000	2050000000	91800000	73439	2040
2000	5	2	0.0036	456000000	20400000	2280000000	102000000	73439	2040
3000	1	2	0.0036	162000000	18600000	162000000	18600000	67109	1860
3000	1.5	2	0.0036	162000000	18600000	243000000	28000000	67109	1860
3000	2	2	0.0036	162000000	18600000	324000000	37300000	67109	1860
3000	2.5	2	0.0036	162000000	18600000	405000000	46600000	67109	1860
3000	3	2	0.0036	162000000	18600000	485000000	55900000	67109	1860
3000	3.5	2	0.0036	162000000	18600000	566000000	65200000	67109	1860
3000	4	2	0.0036	162000000	18600000	647000000	74600000	67109	1860
3000	4.5	2	0.0036	162000000	18600000	728000000	83900000	67109	1860
3000	5	2	0.0036	162000000	18600000	809000000	93200000	67109	1860
4000	1	2	0.0036	75100000	16800000	75100000	16800000	60333	1680
4000	1.5	2	0.0036	75100000	16800000	113000000	25100000	60333	1680
4000	2	2	0.0036	75100000	16800000	150000000	33500000	60333	1680
4000	2.5	2	0.0036	75100000	16800000	188000000	41900000	60333	1680
4000	3	2	0.0036	75100000	16800000	225000000	50300000	60333	1680
4000	3.5	2	0.0036	75100000	16800000	263000000	58700000	60333	1680
4000	4	2	0.0036	75100000	16800000	300000000	67000000	60333	1680
4000	4.5	2	0.0036	75100000	16800000	338000000	75400000	60333	1680
4000	5	2	0.0036	75100000	16800000	375000000	83800000	60333	1680
5000	1	2	0.0036	40400000	14300000	40400000	14300000	51313	1430
5000	1.5	2	0.0036	40400000	14300000	60500000	21400000	51313	1430
5000	2	2	0.0036	40400000	14300000	80700000	28500000	51313	1430
5000	2.5	2	0.0036	40400000	14300000	101000000	35600000	51313	1430
5000	3	2	0.0036	40400000	14300000	121000000	42800000	51313	1430
5000	3.5	2	0.0036	40400000	14300000	141000000	49900000	51313	1430
5000	4	2	0.0036	40400000	14300000	161000000	57000000	51313	1430
5000	4.5	2	0.0036	40400000	14300000	182000000	64100000	51313	1430
5000	5	2	0.0036	40400000	14300000	202000000	71300000	51313	1430
6000	1	2	0.0036	23800000	11400000	23800000	11400000	41092	1140
6000	1.5	2	0.0036	23800000	11400000	35800000	17100000	41092	1140
6000	2	2	0.0036	23800000	11400000	47700000	22800000	41092	1140
6000	2.5	2	0.0036	23800000	11400000	59600000	28500000	41092	1140
6000	3	2	0.0036	23800000	11400000	71500000	34200000	41092	1140
6000	3.5	2	0.0036	23800000	11400000	83400000	40000000	41092	1140
6000	4	2	0.0036	23800000	11400000	95400000	45700000	41092	1140
6000	4.5	2	0.0036	23800000	11400000	107000000	51400000	41092	1140
6000	5	2	0.0036	23800000	11400000	119000000	57100000	41092	1140
7000	1	2	0.0036	15000000	8800000	15000000	8800000	31670	880
7000	1.5	2	0.0036	15000000	8800000	22500000	13200000	31670	880
7000	2	2	0.0036	15000000	8800000	30100000	17600000	31670	880

Slant	Dwell	Atm	Bucket	Peak	Average	Peak F	Average F	PIB	Avg W/Cm2
7000	2.5	2	0.0036	15000000	8800000	37600000	22000000	31670	880
7000	3	2	0.0036	15000000	8800000	45100000	26400000	31670	880
7000	3.5	2	0.0036	15000000	8800000	52600000	30800000	31670	880
7000	4	2	0.0036	15000000	8800000	60100000	35200000	31670	880
7000	4.5	2	0.0036	15000000	8800000	67600000	39600000	31670	880
7000	5	2	0.0036	15000000	8800000	75200000	44000000	31670	880
8000	1	2	0.0036	9940000	6660000	9940000	6660000	23973	666
8000	1.5	2	0.0036	9940000	6660000	14900000	9990000	23973	666
8000	2	2	0.0036	9940000	6660000	19900000	13300000	23973	666
8000	2.5	2	0.0036	9940000	6660000	24900000	16600000	23973	666
8000	3	2	0.0036	9940000	6660000	29800000	20000000	23973	666
8000	3.5	2	0.0036	9940000	6660000	34800000	23300000	23973	666
8000	4	2	0.0036	9940000	6660000	39800000	26600000	23973	666
8000	4.5	2	0.0036	9940000	6660000	44700000	30000000	23973	666
8000	5	2	0.0036	9940000	6660000	49700000	33300000	23973	666
9000	1	2	0.0036	6820000	5010000	6820000	5010000	18053	501
9000	1.5	2	0.0036	6820000	5010000	10200000	7520000	18053	501
9000	2	2	0.0036	6820000	5010000	13600000	10000000	18053	501
9000	2.5	2	0.0036	6820000	5010000	17000000	12500000	18053	501
9000	3	2	0.0036	6820000	5010000	20500000	15000000	18053	501
9000	3.5	2	0.0036	6820000	5010000	23900000	17600000	18053	501
9000	4	2	0.0036	6820000	5010000	27300000	20100000	18053	501
9000	4.5	2	0.0036	6820000	5010000	30700000	22600000	18053	501
9000	5	2	0.0036	6820000	5010000	34100000	25100000	18053	501
10000	1	2	0.0036	4810000	3780000	4810000	3780000	13619	378
10000	1.5	2	0.0036	4810000	3780000	7220000	5670000	13619	378
10000	2	2	0.0036	4810000	3780000	9630000	7570000	13619	378
10000	2.5	2	0.0036	4810000	3780000	12000000	9460000	13619	378
10000	3	2	0.0036	4810000	3780000	14400000	11300000	13619	378
10000	3.5	2	0.0036	4810000	3780000	16800000	13200000	13619	378
10000	4	2	0.0036	4810000	3780000	19300000	15100000	13619	378
10000	4.5	2	0.0036	4810000	3780000	21700000	17000000	13619	378
10000	5	2	0.0036	4810000	3780000	24100000	18900000	13619	378
11000	1	2	0.0036	3480000	2870000	3480000	2870000	10329	287
11000	1.5	2	0.0036	3480000	2870000	5220000	4300000	10329	287
11000	2	2	0.0036	3480000	2870000	6960000	5740000	10329	287
11000	2.5	2	0.0036	3480000	2870000	8700000	7170000	10329	287
11000	3	2	0.0036	3480000	2870000	10400000	8610000	10329	287
11000	3.5	2	0.0036	3480000	2870000	12200000	10000000	10329	287
11000	4	2	0.0036	3480000	2870000	13900000	11500000	10329	287
11000	4.5	2	0.0036	3480000	2870000	15700000	12900000	10329	287
11000	5	2	0.0036	3480000	2870000	17400000	14300000	10329	287
12000	1	2	0.0036	2560000	2190000	2560000	2190000	7889.6	219
12000	1.5	2	0.0036	2560000	2190000	3840000	3290000	7889.6	219
12000	2	2	0.0036	2560000	2190000	5120000	4380000	7889.6	219
12000	2.5	2	0.0036	2560000	2190000	6410000	5480000	7889.6	219
12000	3	2	0.0036	2560000	2190000	7690000	6570000	7889.6	219
12000	3.5	2	0.0036	2560000	2190000	8970000	7670000	7889.6	219
12000	4	2	0.0036	2560000	2190000	10200000	8770000	7889.6	219
12000	4.5	2	0.0036	2560000	2190000	11500000	9860000	7889.6	219
12000	5	2	0.0036	2560000	2190000	12800000	11000000	7889.6	219

Slant	Dwell	Atm	Bucket	Peak	Average	Peak F	Average F	PIB	Avg W/Cm2
2000	1	3	0.0036	661000000	18400000	661000000	18400000	66366	1840
2000	1.5	3	0.0036	661000000	18400000	991000000	27700000	66366	1840
2000	2	3	0.0036	661000000	18400000	1320000000	36900000	66366	1840
2000	2.5	3	0.0036	661000000	18400000	1650000000	46100000	66366	1840
2000	3	3	0.0036	661000000	18400000	1980000000	55300000	66366	1840
2000	3.5	3	0.0036	661000000	18400000	2310000000	64500000	66366	1840
2000	4	3	0.0036	661000000	18400000	2640000000	73700000	66366	1840
2000	4.5	3	0.0036	661000000	18400000	2970000000	83000000	66366	1840
2000	5	3	0.0036	661000000	18400000	3300000000	92200000	66366	1840
3000	1	3	0.0036	224000000	16000000	224000000	16000000	57659	1600
3000	1.5	3	0.0036	224000000	16000000	336000000	24000000	57659	1600
3000	2	3	0.0036	224000000	16000000	448000000	32000000	57659	1600
3000	2.5	3	0.0036	224000000	16000000	560000000	40000000	57659	1600
3000	3	3	0.0036	224000000	16000000	672000000	48000000	57659	1600
3000	3.5	3	0.0036	224000000	16000000	784000000	56100000	57659	1600
3000	4	3	0.0036	224000000	16000000	896000000	64100000	57659	1600
3000	4.5	3	0.0036	224000000	16000000	1010000000	72100000	57659	1600
3000	5	3	0.0036	224000000	16000000	1120000000	80100000	57659	1600
4000	1	3	0.0036	99200000	13900000	99200000	13900000	50013	1390
4000	1.5	3	0.0036	99200000	13900000	149000000	20800000	50013	1390
4000	2	3	0.0036	99200000	13900000	198000000	27800000	50013	1390
4000	2.5	3	0.0036	99200000	13900000	248000000	34700000	50013	1390
4000	3	3	0.0036	99200000	13900000	298000000	41700000	50013	1390
4000	3.5	3	0.0036	99200000	13900000	347000000	48600000	50013	1390
4000	4	3	0.0036	99200000	13900000	397000000	55600000	50013	1390
4000	4.5	3	0.0036	99200000	13900000	446000000	62500000	50013	1390
4000	5	3	0.0036	99200000	13900000	496000000	69500000	50013	1390
5000	1	3	0.0036	50900000	11800000	50900000	11800000	42646	1180
5000	1.5	3	0.0036	50900000	11800000	76300000	17800000	42646	1180
5000	2	3	0.0036	50900000	11800000	102000000	23700000	42646	1180
5000	2.5	3	0.0036	50900000	11800000	127000000	29600000	42646	1180
5000	3	3	0.0036	50900000	11800000	153000000	35500000	42646	1180
5000	3.5	3	0.0036	50900000	11800000	178000000	41500000	42646	1180
5000	4	3	0.0036	50900000	11800000	204000000	47400000	42646	1180
5000	4.5	3	0.0036	50900000	11800000	229000000	53300000	42646	1180
5000	5	3	0.0036	50900000	11800000	254000000	59200000	42646	1180
6000	1	3	0.0036	28700000	9710000	28700000	9710000	34968	971
6000	1.5	3	0.0036	28700000	9710000	43000000	14600000	34968	971
6000	2	3	0.0036	28700000	9710000	57400000	19400000	34968	971
6000	2.5	3	0.0036	28700000	9710000	71700000	24300000	34968	971
6000	3	3	0.0036	28700000	9710000	86000000	29100000	34968	971
6000	3.5	3	0.0036	28700000	9710000	100000000	34000000	34968	971
6000	4	3	0.0036	28700000	9710000	115000000	38900000	34968	971
6000	4.5	3	0.0036	28700000	9710000	129000000	43700000	34968	971
6000	5	3	0.0036	28700000	9710000	143000000	48600000	34968	971
7000	1	3	0.0036	17200000	7640000	17200000	7640000	27509	764

Slant	Dwell	Atm	Bucket	Peak	Average	Peak F	Average F	PIB	Avg W/Cm2
7000	1.5	3	0.0036	17200000	7640000	25900000	11500000	27509	764
7000	2	3	0.0036	17200000	7640000	34500000	15300000	27509	764
7000	2.5	3	0.0036	17200000	7640000	43100000	19100000	27509	764
7000	3	3	0.0036	17200000	7640000	51700000	22900000	27509	764
7000	3.5	3	0.0036	17200000	7640000	60300000	26700000	27509	764
7000	4	3	0.0036	17200000	7640000	69000000	30600000	27509	764
7000	4.5	3	0.0036	17200000	7640000	77600000	34400000	27509	764
7000	5	3	0.0036	17200000	7640000	86200000	38200000	27509	764
8000	1	3	0.0036	10900000	5830000	10900000	5830000	21002	583
8000	1.5	3	0.0036	10900000	5830000	16300000	8750000	21002	583
8000	2	3	0.0036	10900000	5830000	21700000	11700000	21002	583
8000	2.5	3	0.0036	10900000	5830000	27200000	14600000	21002	583
8000	3	3	0.0036	10900000	5830000	32600000	17500000	21002	583
8000	3.5	3	0.0036	10900000	5830000	38100000	20400000	21002	583
8000	4	3	0.0036	10900000	5830000	43500000	23300000	21002	583
8000	4.5	3	0.0036	10900000	5830000	48900000	26300000	21002	583
8000	5	3	0.0036	10900000	5830000	54400000	29200000	21002	583
9000	1	3	0.0036	7110000	4380000	7110000	4380000	15754	438
9000	1.5	3	0.0036	7110000	4380000	10700000	6560000	15754	438
9000	2	3	0.0036	7110000	4380000	14200000	8750000	15754	438
9000	2.5	3	0.0036	7110000	4380000	17800000	10900000	15754	438
9000	3	3	0.0036	7110000	4380000	21300000	13100000	15754	438
9000	3.5	3	0.0036	7110000	4380000	24900000	15300000	15754	438
9000	4	3	0.0036	7110000	4380000	28400000	17500000	15754	438
9000	4.5	3	0.0036	7110000	4380000	32000000	19700000	15754	438
9000	5	3	0.0036	7110000	4380000	35500000	21900000	15754	438
10000	1	3	0.0036	4780000	3260000	4780000	3260000	11718	326
10000	1.5	3	0.0036	4780000	3260000	7170000	4880000	11718	326
10000	2	3	0.0036	4780000	3260000	9570000	6510000	11718	326
10000	2.5	3	0.0036	4780000	3260000	12000000	8140000	11718	326
10000	3	3	0.0036	4780000	3260000	14400000	9760000	11718	326
10000	3.5	3	0.0036	4780000	3260000	16700000	11400000	11718	326
10000	4	3	0.0036	4780000	3260000	19100000	13000000	11718	326
10000	4.5	3	0.0036	4780000	3260000	21500000	14600000	11718	326
10000	5	3	0.0036	4780000	3260000	23900000	16300000	11718	326
11000	1	3	0.0036	3290000	2420000	3290000	2420000	8693.9	242
11000	1.5	3	0.0036	3290000	2420000	4940000	3620000	8693.9	242
11000	2	3	0.0036	3290000	2420000	6590000	4830000	8693.9	242
11000	2.5	3	0.0036	3290000	2420000	8240000	6040000	8693.9	242
11000	3	3	0.0036	3290000	2420000	9880000	7240000	8693.9	242
11000	3.5	3	0.0036	3290000	2420000	11500000	8450000	8693.9	242
11000	4	3	0.0036	3290000	2420000	13200000	9660000	8693.9	242
11000	4.5	3	0.0036	3290000	2420000	14800000	10900000	8693.9	242
11000	5	3	0.0036	3290000	2420000	16500000	12100000	8693.9	242
12000	1	3	0.0036	2310000	1790000	2310000	1790000	6457.1	179
12000	1.5	3	0.0036	2310000	1790000	3470000	2690000	6457.1	179
12000	2	3	0.0036	2310000	1790000	4620000	3590000	6457.1	179
12000	2.5	3	0.0036	2310000	1790000	5780000	4480000	6457.1	179
12000	3	3	0.0036	2310000	1790000	6940000	5380000	6457.1	179

Slant	Dwell	Atm	Bucket	Peak	Average	Peak F	Average F	PIB	Avg W/Cm2
12000	3.5	3	0.0036	2310000	1790000	8090000	6280000	6457.1	179
12000	4	3	0.0036	2310000	1790000	9250000	7170000	6457.1	179
12000	4.5	3	0.0036	2310000	1790000	10400000	8070000	6457.1	179
12000	5	3	0.0036	2310000	1790000	11600000	8970000	6457.1	179
2000	1	4	0.0036	617000000	19300000	617000000	19300000	69646	1930
2000	1.5	4	0.0036	617000000	19300000	926000000	29000000	69646	1930
2000	2	4	0.0036	617000000	19300000	1230000000	38700000	69646	1930
2000	2.5	4	0.0036	617000000	19300000	1540000000	48400000	69646	1930
2000	3	4	0.0036	617000000	19300000	1850000000	58000000	69646	1930
2000	3.5	4	0.0036	617000000	19300000	2160000000	67700000	69646	1930
2000	4	4	0.0036	617000000	19300000	2470000000	77400000	69646	1930
2000	4.5	4	0.0036	617000000	19300000	2780000000	87100000	69646	1930
2000	5	4	0.0036	617000000	19300000	3090000000	96700000	69646	1930
3000	1	4	0.0036	212000000	17200000	212000000	17200000	61993	1720
3000	1.5	4	0.0036	212000000	17200000	318000000	25800000	61993	1720
3000	2	4	0.0036	212000000	17200000	424000000	34400000	61993	1720
3000	2.5	4	0.0036	212000000	17200000	530000000	43100000	61993	1720
3000	3	4	0.0036	212000000	17200000	636000000	51700000	61993	1720
3000	3.5	4	0.0036	212000000	17200000	742000000	60300000	61993	1720
3000	4	4	0.0036	212000000	17200000	848000000	68900000	61993	1720
3000	4.5	4	0.0036	212000000	17200000	954000000	77500000	61993	1720
3000	5	4	0.0036	212000000	17200000	1060000000	86100000	61993	1720
4000	1	4	0.0036	95300000	15300000	95300000	15300000	54988	1530
4000	1.5	4	0.0036	95300000	15300000	143000000	22900000	54988	1530
4000	2	4	0.0036	95300000	15300000	191000000	30500000	54988	1530
4000	2.5	4	0.0036	95300000	15300000	238000000	38200000	54988	1530
4000	3	4	0.0036	95300000	15300000	286000000	45800000	54988	1530
4000	3.5	4	0.0036	95300000	15300000	334000000	53500000	54988	1530
4000	4	4	0.0036	95300000	15300000	381000000	61100000	54988	1530
4000	4.5	4	0.0036	95300000	15300000	429000000	68700000	54988	1530
4000	5	4	0.0036	95300000	15300000	477000000	76400000	54988	1530
5000	1	4	0.0036	49800000	13200000	49800000	13200000	47497	1320
5000	1.5	4	0.0036	49800000	13200000	74700000	19800000	47497	1320
5000	2	4	0.0036	49800000	13200000	99600000	26400000	47497	1320
5000	2.5	4	0.0036	49800000	13200000	124000000	33000000	47497	1320
5000	3	4	0.0036	49800000	13200000	149000000	39600000	47497	1320
5000	3.5	4	0.0036	49800000	13200000	174000000	46200000	47497	1320
5000	4	4	0.0036	49800000	13200000	199000000	52800000	47497	1320
5000	4.5	4	0.0036	49800000	13200000	224000000	59400000	47497	1320
5000	5	4	0.0036	49800000	13200000	249000000	66000000	47497	1320
6000	1	4	0.0036	28600000	10900000	28600000	10900000	39089	1090
6000	1.5	4	0.0036	28600000	10900000	42900000	16300000	39089	1090
6000	2	4	0.0036	28600000	10900000	57200000	21700000	39089	1090
6000	2.5	4	0.0036	28600000	10900000	71500000	27100000	39089	1090
6000	3	4	0.0036	28600000	10900000	85800000	32600000	39089	1090
6000	3.5	4	0.0036	28600000	10900000	100000000	38000000	39089	1090
6000	4	4	0.0036	28600000	10900000	114000000	43400000	39089	1090
6000	4.5	4	0.0036	28600000	10900000	129000000	48900000	39089	1090
6000	5	4	0.0036	28600000	10900000	143000000	54300000	39089	1090
7000	1	4	0.0036	17500000	8560000	17500000	8560000	30798	856

Slant	Dwell	Atm	Bucket	Peak	Average	Peak F	Average F	PIB	Avg W/Cm2
7000	1.5	4	0.0036	17500000	8560000	26300000	12800000	30798	856
7000	2	4	0.0036	17500000	8560000	35100000	17100000	30798	856
7000	2.5	4	0.0036	17500000	8560000	43800000	21400000	30798	856
7000	3	4	0.0036	17500000	8560000	52600000	25700000	30798	856
7000	3.5	4	0.0036	17500000	8560000	61400000	29900000	30798	856
7000	4	4	0.0036	17500000	8560000	70100000	34200000	30798	856
7000	4.5	4	0.0036	17500000	8560000	78900000	38500000	30798	856
7000	5	4	0.0036	17500000	8560000	87700000	42800000	30798	856
8000	1	4	0.0036	11300000	6560000	11300000	6560000	23598	656
8000	1.5	4	0.0036	11300000	6560000	16900000	9830000	23598	656
8000	2	4	0.0036	11300000	6560000	22600000	13100000	23598	656
8000	2.5	4	0.0036	11300000	6560000	28200000	16400000	23598	656
8000	3	4	0.0036	11300000	6560000	33900000	19700000	23598	656
8000	3.5	4	0.0036	11300000	6560000	39500000	22900000	23598	656
8000	4	4	0.0036	11300000	6560000	45100000	26200000	23598	656
8000	4.5	4	0.0036	11300000	6560000	50800000	29500000	23598	656
8000	5	4	0.0036	11300000	6560000	56400000	32800000	23598	656
9000	1	4	0.0036	7540000	4950000	7540000	4950000	17825	495
9000	1.5	4	0.0036	7540000	4950000	11300000	7430000	17825	495
9000	2	4	0.0036	7540000	4950000	15100000	9900000	17825	495
9000	2.5	4	0.0036	7540000	4950000	18800000	12400000	17825	495
9000	3	4	0.0036	7540000	4950000	22600000	14900000	17825	495
9000	3.5	4	0.0036	7540000	4950000	26400000	17300000	17825	495
9000	4	4	0.0036	7540000	4950000	30200000	19800000	17825	495
9000	4.5	4	0.0036	7540000	4950000	33900000	22300000	17825	495
9000	5	4	0.0036	7540000	4950000	37700000	24800000	17825	495
10000	1	4	0.0036	5180000	3720000	5180000	3720000	13394	372
10000	1.5	4	0.0036	5180000	3720000	7770000	5580000	13394	372
10000	2	4	0.0036	5180000	3720000	10400000	7440000	13394	372
10000	2.5	4	0.0036	5180000	3720000	13000000	9300000	13394	372
10000	3	4	0.0036	5180000	3720000	15500000	11200000	13394	372
10000	3.5	4	0.0036	5180000	3720000	18100000	13000000	13394	372
10000	4	4	0.0036	5180000	3720000	20700000	14900000	13394	372
10000	4.5	4	0.0036	5180000	3720000	23300000	16700000	13394	372
10000	5	4	0.0036	5180000	3720000	25900000	18600000	13394	372
11000	1	4	0.0036	3650000	2800000	3650000	2800000	10067	280
11000	1.5	4	0.0036	3650000	2800000	5470000	4190000	10067	280
11000	2	4	0.0036	3650000	2800000	7300000	5590000	10067	280
11000	2.5	4	0.0036	3650000	2800000	9120000	6990000	10067	280
11000	3	4	0.0036	3650000	2800000	10900000	8390000	10067	280
11000	3.5	4	0.0036	3650000	2800000	12800000	9790000	10067	280
11000	4	4	0.0036	3650000	2800000	14600000	11200000	10067	280
11000	4.5	4	0.0036	3650000	2800000	16400000	12600000	10067	280
11000	5	4	0.0036	3650000	2800000	18200000	14000000	10067	280
12000	1	4	0.0036	2620000	2110000	2620000	2110000	7590.5	211
12000	1.5	4	0.0036	2620000	2110000	3930000	3160000	7590.5	211
12000	2	4	0.0036	2620000	2110000	5240000	4220000	7590.5	211
12000	2.5	4	0.0036	2620000	2110000	6550000	5270000	7590.5	211
12000	3	4	0.0036	2620000	2110000	7860000	6330000	7590.5	211

Slant	Dwell	Atm	Bucket	Peak	Average	Peak F	Average F	PIB	Avg W/Cm2
12000	3.5	4	0.0036	2620000	2110000	9170000	7380000	7590.5	211
12000	4	4	0.0036	2620000	2110000	10500000	8430000	7590.5	211
12000	4.5	4	0.0036	2620000	2110000	11800000	9490000	7590.5	211
12000	5	4	0.0036	2620000	2110000	13100000	10500000	7590.5	211
2000	1	5	0.0036	636000000	20300000	636000000	20300000	73108	2030
2000	1.5	5	0.0036	636000000	20300000	954000000	30500000	73108	2030
2000	2	5	0.0036	636000000	20300000	1270000000	40600000	73108	2030
2000	2.5	5	0.0036	636000000	20300000	1590000000	50800000	73108	2030
2000	3	5	0.0036	636000000	20300000	1910000000	60900000	73108	2030
2000	3.5	5	0.0036	636000000	20300000	2230000000	71100000	73108	2030
2000	4	5	0.0036	636000000	20300000	2540000000	81200000	73108	2030
2000	4.5	5	0.0036	636000000	20300000	2860000000	91400000	73108	2030
2000	5	5	0.0036	636000000	20300000	3180000000	102000000	73108	2030
3000	1	5	0.0036	223000000	18500000	223000000	18500000	66678	1850
3000	1.5	5	0.0036	223000000	18500000	334000000	27800000	66678	1850
3000	2	5	0.0036	223000000	18500000	445000000	37000000	66678	1850
3000	2.5	5	0.0036	223000000	18500000	557000000	46300000	66678	1850
3000	3	5	0.0036	223000000	18500000	668000000	55600000	66678	1850
3000	3.5	5	0.0036	223000000	18500000	779000000	64800000	66678	1850
3000	4	5	0.0036	223000000	18500000	890000000	74100000	66678	1850
3000	4.5	5	0.0036	223000000	18500000	1000000000	83300000	66678	1850
3000	5	5	0.0036	223000000	18500000	1110000000	92600000	66678	1850
4000	1	5	0.0036	102000000	16800000	102000000	16800000	60567	1680
4000	1.5	5	0.0036	102000000	16800000	153000000	25200000	60567	1680
4000	2	5	0.0036	102000000	16800000	204000000	33600000	60567	1680
4000	2.5	5	0.0036	102000000	16800000	255000000	42100000	60567	1680
4000	3	5	0.0036	102000000	16800000	306000000	50500000	60567	1680
4000	3.5	5	0.0036	102000000	16800000	358000000	58900000	60567	1680
4000	4	5	0.0036	102000000	16800000	409000000	67300000	60567	1680
4000	4.5	5	0.0036	102000000	16800000	460000000	75700000	60567	1680
4000	5	5	0.0036	102000000	16800000	511000000	84100000	60567	1680
5000	1	5	0.0036	54400000	14800000	54400000	14800000	53438	1480
5000	1.5	5	0.0036	54400000	14800000	81700000	22300000	53438	1480
5000	2	5	0.0036	54400000	14800000	109000000	29700000	53438	1480
5000	2.5	5	0.0036	54400000	14800000	136000000	37100000	53438	1480
5000	3	5	0.0036	54400000	14800000	163000000	44500000	53438	1480
5000	3.5	5	0.0036	54400000	14800000	191000000	52000000	53438	1480
5000	4	5	0.0036	54400000	14800000	218000000	59400000	53438	1480
5000	4.5	5	0.0036	54400000	14800000	245000000	66800000	53438	1480
5000	5	5	0.0036	54400000	14800000	272000000	74200000	53438	1480
6000	1	5	0.0036	31900000	12400000	31900000	12400000	44806	1240
6000	1.5	5	0.0036	31900000	12400000	47900000	18700000	44806	1240
6000	2	5	0.0036	31900000	12400000	63800000	24900000	44806	1240
6000	2.5	5	0.0036	31900000	12400000	79800000	31100000	44806	1240
6000	3	5	0.0036	31900000	12400000	95800000	37300000	44806	1240
6000	3.5	5	0.0036	31900000	12400000	112000000	43600000	44806	1240
6000	4	5	0.0036	31900000	12400000	128000000	49800000	44806	1240
6000	4.5	5	0.0036	31900000	12400000	144000000	56000000	44806	1240
6000	5	5	0.0036	31900000	12400000	160000000	62200000	44806	1240

Slant	Dwell	Atm	Bucket	Peak	Average	Peak F	Average F	PIB	Avg W/Cm2
7000	1	5	0.0036	20000000	9980000	20000000	9980000	35932	998
7000	1.5	5	0.0036	20000000	9980000	30000000	15000000	35932	998
7000	2	5	0.0036	20000000	9980000	40000000	20000000	35932	998
7000	2.5	5	0.0036	20000000	9980000	50000000	25000000	35932	998
7000	3	5	0.0036	20000000	9980000	60000000	29900000	35932	998
7000	3.5	5	0.0036	20000000	9980000	70000000	34900000	35932	998
7000	4	5	0.0036	20000000	9980000	80000000	39900000	35932	998
7000	4.5	5	0.0036	20000000	9980000	90000000	44900000	35932	998
7000	5	5	0.0036	20000000	9980000	99900000	49900000	35932	998
8000	1	5	0.0036	13100000	7790000	13100000	7790000	28027	779
8000	1.5	5	0.0036	13100000	7790000	19700000	11700000	28027	779
8000	2	5	0.0036	13100000	7790000	26300000	15600000	28027	779
8000	2.5	5	0.0036	13100000	7790000	32900000	19500000	28027	779
8000	3	5	0.0036	13100000	7790000	39400000	23400000	28027	779
8000	3.5	5	0.0036	13100000	7790000	46000000	27200000	28027	779
8000	4	5	0.0036	13100000	7790000	52600000	31100000	28027	779
8000	4.5	5	0.0036	13100000	7790000	59100000	35000000	28027	779
8000	5	5	0.0036	13100000	7790000	65700000	38900000	28027	779
9000	1	5	0.0036	8960000	5990000	8960000	5990000	21564	599
9000	1.5	5	0.0036	8960000	5990000	13400000	8980000	21564	599
9000	2	5	0.0036	8960000	5990000	17900000	12000000	21564	599
9000	2.5	5	0.0036	8960000	5990000	22400000	15000000	21564	599
9000	3	5	0.0036	8960000	5990000	26900000	18000000	21564	599
9000	3.5	5	0.0036	8960000	5990000	31400000	21000000	21564	599
9000	4	5	0.0036	8960000	5990000	35900000	24000000	21564	599
9000	4.5	5	0.0036	8960000	5990000	40300000	27000000	21564	599
9000	5	5	0.0036	8960000	5990000	44800000	30000000	21564	599
10000	1	5	0.0036	6300000	4590000	6300000	4590000	16515	459
10000	1.5	5	0.0036	6300000	4590000	9450000	6880000	16515	459
10000	2	5	0.0036	6300000	4590000	12600000	9170000	16515	459
10000	2.5	5	0.0036	6300000	4590000	15700000	11500000	16515	459
10000	3	5	0.0036	6300000	4590000	18900000	13800000	16515	459
10000	3.5	5	0.0036	6300000	4590000	22000000	16100000	16515	459
10000	4	5	0.0036	6300000	4590000	25200000	18400000	16515	459
10000	4.5	5	0.0036	6300000	4590000	28300000	20600000	16515	459
10000	5	5	0.0036	6300000	4590000	31500000	22900000	16515	459
11000	1	5	0.0036	4530000	3520000	4530000	3520000	12658	352
11000	1.5	5	0.0036	4530000	3520000	6800000	5270000	12658	352
11000	2	5	0.0036	4530000	3520000	9060000	7030000	12658	352
11000	2.5	5	0.0036	4530000	3520000	11300000	8790000	12658	352
11000	3	5	0.0036	4530000	3520000	13600000	10500000	12658	352
11000	3.5	5	0.0036	4530000	3520000	15900000	12300000	12658	352
11000	4	5	0.0036	4530000	3520000	18100000	14100000	12658	352
11000	4.5	5	0.0036	4530000	3520000	20400000	15800000	12658	352
11000	5	5	0.0036	4530000	3520000	22700000	17600000	12658	352
12000	1	5	0.0036	3320000	2710000	3320000	2710000	9738.2	271
12000	1.5	5	0.0036	3320000	2710000	4990000	4060000	9738.2	271
12000	2	5	0.0036	3320000	2710000	6650000	5410000	9738.2	271
12000	2.5	5	0.0036	3320000	2710000	8310000	6760000	9738.2	271

Slant	Dwell	Atm	Bucket	Peak	Average	Peak F	Average F	PIB	Avg W/Cm2
12000	3	5	0.0036	3320000	2710000	9970000	8120000	9738.2	271
12000	3.5	5	0.0036	3320000	2710000	11600000	9470000	9738.2	271
12000	4	5	0.0036	3320000	2710000	13300000	10800000	9738.2	271
12000	4.5	5	0.0036	3320000	2710000	15000000	12200000	9738.2	271
12000	5	5	0.0036	3320000	2710000	16600000	13500000	9738.2	271
2000	1	6	0.0036	636000000	20300000	636000000	20300000	73108	2030
2000	1.5	6	0.0036	636000000	20300000	954000000	30500000	73108	2030
2000	2	6	0.0036	636000000	20300000	1270000000	40600000	73108	2030
2000	2.5	6	0.0036	636000000	20300000	1590000000	50800000	73108	2030
2000	3	6	0.0036	636000000	20300000	1910000000	60900000	73108	2030
2000	3.5	6	0.0036	636000000	20300000	2230000000	71100000	73108	2030
2000	4	6	0.0036	636000000	20300000	2540000000	81200000	73108	2030
2000	4.5	6	0.0036	636000000	20300000	2860000000	91400000	73108	2030
2000	5	6	0.0036	636000000	20300000	3180000000	102000000	73108	2030
3000	1	6	0.0036	223000000	18500000	223000000	18500000	66678	1850
3000	1.5	6	0.0036	223000000	18500000	334000000	27800000	66678	1850
3000	2	6	0.0036	223000000	18500000	445000000	37000000	66678	1850
3000	2.5	6	0.0036	223000000	18500000	557000000	46300000	66678	1850
3000	3	6	0.0036	223000000	18500000	668000000	55600000	66678	1850
3000	3.5	6	0.0036	223000000	18500000	779000000	64800000	66678	1850
3000	4	6	0.0036	223000000	18500000	890000000	74100000	66678	1850
3000	4.5	6	0.0036	223000000	18500000	1000000000	83300000	66678	1850
3000	5	6	0.0036	223000000	18500000	1110000000	92600000	66678	1850
4000	1	6	0.0036	102000000	16800000	102000000	16800000	60567	1680
4000	1.5	6	0.0036	102000000	16800000	153000000	25200000	60567	1680
4000	2	6	0.0036	102000000	16800000	204000000	33600000	60567	1680
4000	2.5	6	0.0036	102000000	16800000	255000000	42100000	60567	1680
4000	3	6	0.0036	102000000	16800000	306000000	50500000	60567	1680
4000	3.5	6	0.0036	102000000	16800000	358000000	58900000	60567	1680
4000	4	6	0.0036	102000000	16800000	409000000	67300000	60567	1680
4000	4.5	6	0.0036	102000000	16800000	460000000	75700000	60567	1680
4000	5	6	0.0036	102000000	16800000	511000000	84100000	60567	1680
5000	1	6	0.0036	54400000	14800000	54400000	14800000	53438	1480
5000	1.5	6	0.0036	54400000	14800000	81700000	22300000	53438	1480
5000	2	6	0.0036	54400000	14800000	109000000	29700000	53438	1480
5000	2.5	6	0.0036	54400000	14800000	136000000	37100000	53438	1480
5000	3	6	0.0036	54400000	14800000	163000000	44500000	53438	1480
5000	3.5	6	0.0036	54400000	14800000	191000000	52000000	53438	1480
5000	4	6	0.0036	54400000	14800000	218000000	59400000	53438	1480
5000	4.5	6	0.0036	54400000	14800000	245000000	66800000	53438	1480
5000	5	6	0.0036	54400000	14800000	272000000	74200000	53438	1480
6000	1	6	0.0036	31900000	12400000	31900000	12400000	44806	1240
6000	1.5	6	0.0036	31900000	12400000	47900000	18700000	44806	1240
6000	2	6	0.0036	31900000	12400000	63800000	24900000	44806	1240
6000	2.5	6	0.0036	31900000	12400000	79800000	31100000	44806	1240
6000	3	6	0.0036	31900000	12400000	95800000	37300000	44806	1240
6000	3.5	6	0.0036	31900000	12400000	112000000	43600000	44806	1240
6000	4	6	0.0036	31900000	12400000	128000000	49800000	44806	1240
6000	4.5	6	0.0036	31900000	12400000	144000000	56000000	44806	1240

Slant	Dwell	Atm	Bucket	Peak	Average	Peak F	Average F	PIB	Avg W/Cm2
6000	5	6	0.0036	31900000	12400000	160000000	62200000	44806	1240
7000	1	6	0.0036	20000000	9980000	20000000	9980000	35932	998
7000	1.5	6	0.0036	20000000	9980000	30000000	15000000	35932	998
7000	2	6	0.0036	20000000	9980000	40000000	20000000	35932	998
7000	2.5	6	0.0036	20000000	9980000	50000000	25000000	35932	998
7000	3	6	0.0036	20000000	9980000	60000000	29900000	35932	998
7000	3.5	6	0.0036	20000000	9980000	70000000	34900000	35932	998
7000	4	6	0.0036	20000000	9980000	80000000	39900000	35932	998
7000	4.5	6	0.0036	20000000	9980000	90000000	44900000	35932	998
7000	5	6	0.0036	20000000	9980000	99900000	49900000	35932	998
8000	1	6	0.0036	13100000	7790000	13100000	7790000	28027	779
8000	1.5	6	0.0036	13100000	7790000	19700000	11700000	28027	779
8000	2	6	0.0036	13100000	7790000	26300000	15600000	28027	779
8000	2.5	6	0.0036	13100000	7790000	32900000	19500000	28027	779
8000	3	6	0.0036	13100000	7790000	39400000	23400000	28027	779
8000	3.5	6	0.0036	13100000	7790000	46000000	27200000	28027	779
8000	4	6	0.0036	13100000	7790000	52600000	31100000	28027	779
8000	4.5	6	0.0036	13100000	7790000	59100000	35000000	28027	779
8000	5	6	0.0036	13100000	7790000	65700000	38900000	28027	779
9000	1	6	0.0036	8960000	5990000	8960000	5990000	21564	599
9000	1.5	6	0.0036	8960000	5990000	13400000	8980000	21564	599
9000	2	6	0.0036	8960000	5990000	17900000	12000000	21564	599
9000	2.5	6	0.0036	8960000	5990000	22400000	15000000	21564	599
9000	3	6	0.0036	8960000	5990000	26900000	18000000	21564	599
9000	3.5	6	0.0036	8960000	5990000	31400000	21000000	21564	599
9000	4	6	0.0036	8960000	5990000	35900000	24000000	21564	599
9000	4.5	6	0.0036	8960000	5990000	40300000	27000000	21564	599
9000	5	6	0.0036	8960000	5990000	44800000	30000000	21564	599
10000	1	6	0.0036	6300000	4590000	6300000	4590000	16515	459
10000	1.5	6	0.0036	6300000	4590000	9450000	6880000	16515	459
10000	2	6	0.0036	6300000	4590000	12600000	9170000	16515	459
10000	2.5	6	0.0036	6300000	4590000	15700000	11500000	16515	459
10000	3	6	0.0036	6300000	4590000	18900000	13800000	16515	459
10000	3.5	6	0.0036	6300000	4590000	22000000	16100000	16515	459
10000	4	6	0.0036	6300000	4590000	25200000	18400000	16515	459
10000	4.5	6	0.0036	6300000	4590000	28300000	20600000	16515	459
10000	5	6	0.0036	6300000	4590000	31500000	22900000	16515	459
11000	1	6	0.0036	4530000	3520000	4530000	3520000	12658	352
11000	1.5	6	0.0036	4530000	3520000	6800000	5270000	12658	352
11000	2	6	0.0036	4530000	3520000	9060000	7030000	12658	352
11000	2.5	6	0.0036	4530000	3520000	11300000	8790000	12658	352
11000	3	6	0.0036	4530000	3520000	13600000	10500000	12658	352
11000	3.5	6	0.0036	4530000	3520000	15900000	12300000	12658	352
11000	4	6	0.0036	4530000	3520000	18100000	14100000	12658	352
11000	4.5	6	0.0036	4530000	3520000	20400000	15800000	12658	352
11000	5	6	0.0036	4530000	3520000	22700000	17600000	12658	352
12000	1	6	0.0036	3320000	2710000	3320000	2710000	9738.2	271
12000	1.5	6	0.0036	3320000	2710000	4990000	4060000	9738.2	271
12000	2	6	0.0036	3320000	2710000	6650000	5410000	9738.2	271

Slant	Dwell	Atm	Bucket	Peak	Average	Peak F	Average F	PIB	Avg W/Cm2
12000	2.5	6	0.0036	3320000	2710000	8310000	6760000	9738.2	271
12000	3	6	0.0036	3320000	2710000	9970000	8120000	9738.2	271
12000	3.5	6	0.0036	3320000	2710000	11600000	9470000	9738.2	271
12000	4	6	0.0036	3320000	2710000	13300000	10800000	9738.2	271
12000	4.5	6	0.0036	3320000	2710000	15000000	12200000	9738.2	271
12000	5	6	0.0036	3320000	2710000	16600000	13500000	9738.2	271
2000	1	7	0.0036	762000000	21400000	762000000	21400000	76983	2140
2000	1.5	7	0.0036	762000000	21400000	1140000000	32100000	76983	2140
2000	2	7	0.0036	762000000	21400000	1520000000	42800000	76983	2140
2000	2.5	7	0.0036	762000000	21400000	1900000000	53500000	76983	2140
2000	3	7	0.0036	762000000	21400000	2290000000	64200000	76983	2140
2000	3.5	7	0.0036	762000000	21400000	2670000000	74800000	76983	2140
2000	4	7	0.0036	762000000	21400000	3050000000	85500000	76983	2140
2000	4.5	7	0.0036	762000000	21400000	3430000000	96200000	76983	2140
2000	5	7	0.0036	762000000	21400000	3810000000	107000000	76983	2140
3000	1	7	0.0036	276000000	20000000	276000000	20000000	72049	2000
3000	1.5	7	0.0036	276000000	20000000	414000000	30000000	72049	2000
3000	2	7	0.0036	276000000	20000000	551000000	40000000	72049	2000
3000	2.5	7	0.0036	276000000	20000000	689000000	50000000	72049	2000
3000	3	7	0.0036	276000000	20000000	827000000	60000000	72049	2000
3000	3.5	7	0.0036	276000000	20000000	965000000	70000000	72049	2000
3000	4	7	0.0036	276000000	20000000	1100000000	80100000	72049	2000
3000	4.5	7	0.0036	276000000	20000000	1240000000	90100000	72049	2000
3000	5	7	0.0036	276000000	20000000	1380000000	100000000	72049	2000
4000	1	7	0.0036	130000000	18700000	130000000	18700000	67305	1870
4000	1.5	7	0.0036	130000000	18700000	195000000	28000000	67305	1870
4000	2	7	0.0036	130000000	18700000	260000000	37400000	67305	1870
4000	2.5	7	0.0036	130000000	18700000	326000000	46700000	67305	1870
4000	3	7	0.0036	130000000	18700000	391000000	56100000	67305	1870
4000	3.5	7	0.0036	130000000	18700000	456000000	65400000	67305	1870
4000	4	7	0.0036	130000000	18700000	521000000	74800000	67305	1870
4000	4.5	7	0.0036	130000000	18700000	586000000	84100000	67305	1870
4000	5	7	0.0036	130000000	18700000	651000000	93500000	67305	1870
5000	1	7	0.0036	71300000	17100000	71300000	17100000	61673	1710
5000	1.5	7	0.0036	71300000	17100000	107000000	25700000	61673	1710
5000	2	7	0.0036	71300000	17100000	143000000	34300000	61673	1710
5000	2.5	7	0.0036	71300000	17100000	178000000	42800000	61673	1710
5000	3	7	0.0036	71300000	17100000	214000000	51400000	61673	1710
5000	3.5	7	0.0036	71300000	17100000	250000000	60000000	61673	1710
5000	4	7	0.0036	71300000	17100000	285000000	68500000	61673	1710
5000	4.5	7	0.0036	71300000	17100000	321000000	77100000	61673	1710
5000	5	7	0.0036	71300000	17100000	357000000	85700000	61673	1710
6000	1	7	0.0036	42900000	15000000	42900000	15000000	54134	1500
6000	1.5	7	0.0036	42900000	15000000	64400000	22600000	54134	1500
6000	2	7	0.0036	42900000	15000000	85800000	30100000	54134	1500
6000	2.5	7	0.0036	42900000	15000000	107000000	37600000	54134	1500
6000	3	7	0.0036	42900000	15000000	129000000	45100000	54134	1500
6000	3.5	7	0.0036	42900000	15000000	150000000	52600000	54134	1500
6000	4	7	0.0036	42900000	15000000	172000000	60100000	54134	1500

Slant	Dwell	Atm	Bucket	Peak	Average	Peak F	Average F	PIB	Avg W/Cm2
6000	4.5	7	0.0036	42900000	15000000	193000000	67700000	54134	1500
6000	5	7	0.0036	42900000	15000000	215000000	75200000	54134	1500
7000	1	7	0.0036	27600000	12600000	27600000	12600000	45462	1260
7000	1.5	7	0.0036	27600000	12600000	41300000	18900000	45462	1260
7000	2	7	0.0036	27600000	12600000	55100000	25300000	45462	1260
7000	2.5	7	0.0036	27600000	12600000	68900000	31600000	45462	1260
7000	3	7	0.0036	27600000	12600000	82700000	37900000	45462	1260
7000	3.5	7	0.0036	27600000	12600000	96400000	44200000	45462	1260
7000	4	7	0.0036	27600000	12600000	110000000	50500000	45462	1260
7000	4.5	7	0.0036	27600000	12600000	124000000	56800000	45462	1260
7000	5	7	0.0036	27600000	12600000	138000000	63100000	45462	1260
8000	1	7	0.0036	18600000	10300000	18600000	10300000	37005	1030
8000	1.5	7	0.0036	18600000	10300000	27900000	15400000	37005	1030
8000	2	7	0.0036	18600000	10300000	37100000	20600000	37005	1030
8000	2.5	7	0.0036	18600000	10300000	46400000	25700000	37005	1030
8000	3	7	0.0036	18600000	10300000	55700000	30800000	37005	1030
8000	3.5	7	0.0036	18600000	10300000	65000000	36000000	37005	1030
8000	4	7	0.0036	18600000	10300000	74300000	41100000	37005	1030
8000	4.5	7	0.0036	18600000	10300000	83500000	46300000	37005	1030
8000	5	7	0.0036	18600000	10300000	92800000	51400000	37005	1030
9000	1	7	0.0036	13000000	8220000	13000000	8220000	29591	822
9000	1.5	7	0.0036	13000000	8220000	19500000	12300000	29591	822
9000	2	7	0.0036	13000000	8220000	26000000	16400000	29591	822
9000	2.5	7	0.0036	13000000	8220000	32400000	20500000	29591	822
9000	3	7	0.0036	13000000	8220000	38900000	24700000	29591	822
9000	3.5	7	0.0036	13000000	8220000	45400000	28800000	29591	822
9000	4	7	0.0036	13000000	8220000	51900000	32900000	29591	822
9000	4.5	7	0.0036	13000000	8220000	58400000	37000000	29591	822
9000	5	7	0.0036	13000000	8220000	64900000	41100000	29591	822
10000	1	7	0.0036	9340000	6520000	9340000	6520000	23472	652
10000	1.5	7	0.0036	9340000	6520000	14000000	9780000	23472	652
10000	2	7	0.0036	9340000	6520000	18700000	13000000	23472	652
10000	2.5	7	0.0036	9340000	6520000	23400000	16300000	23472	652
10000	3	7	0.0036	9340000	6520000	28000000	19600000	23472	652
10000	3.5	7	0.0036	9340000	6520000	32700000	22800000	23472	652
10000	4	7	0.0036	9340000	6520000	37400000	26100000	23472	652
10000	4.5	7	0.0036	9340000	6520000	42000000	29300000	23472	652
10000	5	7	0.0036	9340000	6520000	46700000	32600000	23472	652
11000	1	7	0.0036	6880000	5160000	6880000	5160000	18583	516
11000	1.5	7	0.0036	6880000	5160000	10300000	7740000	18583	516
11000	2	7	0.0036	6880000	5160000	13800000	10300000	18583	516
11000	2.5	7	0.0036	6880000	5160000	17200000	12900000	18583	516
11000	3	7	0.0036	6880000	5160000	20600000	15500000	18583	516
11000	3.5	7	0.0036	6880000	5160000	24100000	18100000	18583	516
11000	4	7	0.0036	6880000	5160000	27500000	20600000	18583	516
11000	4.5	7	0.0036	6880000	5160000	31000000	23200000	18583	516
11000	5	7	0.0036	6880000	5160000	34400000	25800000	18583	516
12000	1	7	0.0036	5170000	4090000	5170000	4090000	14738	409
12000	1.5	7	0.0036	5170000	4090000	7760000	6140000	14738	409

Slant	Dwell	Atm	Bucket	Peak	Average	Peak F	Average F	PIB	Avg W/Cm2
12000	2	7	0.0036	5170000	4090000	10300000	8190000	14738	409
12000	2.5	7	0.0036	5170000	4090000	12900000	10200000	14738	409
12000	3	7	0.0036	5170000	4090000	15500000	12300000	14738	409
12000	3.5	7	0.0036	5170000	4090000	18100000	14300000	14738	409
12000	4	7	0.0036	5170000	4090000	20700000	16400000	14738	409
12000	4.5	7	0.0036	5170000	4090000	23300000	18400000	14738	409
12000	5	7	0.0036	5170000	4090000	25900000	20500000	14738	409

Appendix C: Vulnerability Tables

1976 Standard Atmosphere

Atm	Slant Range	Irradiance	Aim 1	Aim 2	Aim 3	Aim 4
1	2000	2225.06	1.2	2.5	2.5	4.9
1	2250	2163.15	1.3	2.5	2.5	5.0
1	2500	2101.99	1.3	2.6	2.6	5.2
1	2750	2041.60	1.3	2.7	2.7	5.3
1	3000	1981.97	1.4	2.8	2.8	5.5
1	3250	1923.11	1.4	2.9	2.9	5.7
1	3500	1865.01	1.5	2.9	2.9	5.8
1	3750	1807.68	1.5	3.0	3.0	6.0
1	4000	1751.10	1.6	3.1	3.1	6.2
1	4250	1695.30	1.6	3.2	3.2	6.4
1	4500	1640.25	1.7	3.4	3.4	6.6
1	4750	1585.97	1.7	3.5	3.5	6.9
1	5000	1532.45	1.8	3.6	3.6	7.1
1	5250	1479.70	1.9	3.7	3.7	7.4
1	5500	1427.71	1.9	3.9	3.9	7.6
1	5750	1376.49	2.0	4.0	4.0	7.9
1	6000	1326.02	2.1	4.1	4.1	8.2
1	6250	1276.33	2.2	4.3	4.3	8.5
1	6500	1227.39	2.2	4.5	4.5	8.9
1	6750	1179.22	2.3	4.7	4.7	9.2
1	7000	1131.81	2.4	4.9	4.9	9.6
1	7250	1085.17	2.5	5.1	5.1	10.0
1	7500	1039.29	2.6	5.3	5.3	10.5
1	7750	994.18	2.8	5.5	5.5	11.0
1	8000	949.82	2.9	5.8	5.8	11.5
1	8250	906.24	3.0	6.1	6.1	12.0
1	8500	863.41	3.2	6.4	6.4	12.6
1	8750	821.35	3.3	6.7	6.7	13.3
1	9000	780.05	3.5	7.1	7.1	14.0
1	9250	739.52	3.7	7.4	7.4	14.7
1	9500	699.75	3.9	7.9	7.9	15.6
1	9750	660.75	4.2	8.3	8.3	16.5
1	10000	622.50	4.4	8.8	8.8	17.5
1	10250	585.03	4.7	9.4	9.4	18.6
1	10500	548.31	5.0	10.0	10.0	19.9
1	10750	512.36	5.4	10.7	10.7	21.3
1	11000	477.17	5.8	11.5	11.5	22.8
1	11250	442.75	6.2	12.4	12.4	24.6
1	11500	409.09	6.7	13.4	13.4	26.6
1	11750	376.20	7.3	14.6	14.6	28.9
1	12000	344.06	8.0	16.0	16.0	31.7

Mid-Latitude Atmosphere

Atm	Slant Range	Irradiance	Aim 1	Aim 2	Aim 3	Aim 4
2	2000	2032.43	1.4	2.7	2.7	5.4
2	2250	1970.51	1.4	2.8	2.8	5.5
2	2500	1909.36	1.4	2.9	2.9	5.7
2	2750	1848.96	1.5	3.0	3.0	5.9
2	3000	1789.34	1.5	3.1	3.1	6.1
2	3250	1730.47	1.6	3.2	3.2	6.3
2	3500	1672.38	1.6	3.3	3.3	6.5
2	3750	1615.04	1.7	3.4	3.4	6.7
2	4000	1558.47	1.8	3.5	3.5	7.0
2	4250	1502.66	1.8	3.7	3.7	7.2
2	4500	1447.62	1.9	3.8	3.8	7.5
2	4750	1393.33	2.0	3.9	3.9	7.8
2	5000	1339.82	2.1	4.1	4.1	8.1
2	5250	1287.06	2.1	4.3	4.3	8.5
2	5500	1235.08	2.2	4.5	4.5	8.8
2	5750	1183.85	2.3	4.6	4.6	9.2
2	6000	1133.39	2.4	4.9	4.9	9.6
2	6250	1083.69	2.5	5.1	5.1	10.0
2	6500	1034.76	2.7	5.3	5.3	10.5
2	6750	986.58	2.8	5.6	5.6	11.0
2	7000	939.18	2.9	5.9	5.9	11.6
2	7250	892.53	3.1	6.2	6.2	12.2
2	7500	846.66	3.2	6.5	6.5	12.9
2	7750	801.54	3.4	6.9	6.9	13.6
2	8000	757.19	3.6	7.3	7.3	14.4
2	8250	713.60	3.9	7.7	7.7	15.3
2	8500	670.78	4.1	8.2	8.2	16.2
2	8750	628.71	4.4	8.7	8.7	17.3
2	9000	587.42	4.7	9.4	9.4	18.5
2	9250	546.88	5.0	10.1	10.1	19.9
2	9500	507.12	5.4	10.8	10.8	21.5
2	9750	468.11	5.9	11.7	11.7	23.3
2	10000	429.87	6.4	12.8	12.8	25.3
2	10250	392.39	7.0	14.0	14.0	27.8
2	10500	355.68	7.7	15.5	15.5	30.6
2	10750	319.72	8.6	17.2	17.2	34.1
2	11000	284.54	9.7	19.3	19.3	38.3
2	11250	250.11	11.0	22.0	22.0	43.5
2	11500	216.46	12.7	25.4	25.4	50.3
2	11750	183.56	15.0	30.0	30.0	59.3
2	12000	151.43	18.2	36.3	36.3	71.9

Langley Atmosphere

Atm	Slant Range	Irradiance	Aim 1	Aim 2	Aim 3	Aim 4
3	2000	1889.88	1.5	2.9	2.9	5.8
3	2250	1827.96	1.5	3.0	3.0	6.0
3	2500	1766.81	1.6	3.1	3.1	6.2
3	2750	1706.42	1.6	3.2	3.2	6.4
3	3000	1646.79	1.7	3.3	3.3	6.6
3	3250	1587.93	1.7	3.5	3.5	6.9
3	3500	1529.83	1.8	3.6	3.6	7.1
3	3750	1472.49	1.9	3.7	3.7	7.4
3	4000	1415.92	1.9	3.9	3.9	7.7
3	4250	1360.11	2.0	4.0	4.0	8.0
3	4500	1305.07	2.1	4.2	4.2	8.3
3	4750	1250.79	2.2	4.4	4.4	8.7
3	5000	1197.27	2.3	4.6	4.6	9.1
3	5250	1144.52	2.4	4.8	4.8	9.5
3	5500	1092.53	2.5	5.0	5.0	10.0
3	5750	1041.30	2.6	5.3	5.3	10.5
3	6000	990.84	2.8	5.6	5.6	11.0
3	6250	941.14	2.9	5.8	5.8	11.6
3	6500	892.21	3.1	6.2	6.2	12.2
3	6750	844.04	3.3	6.5	6.5	12.9
3	7000	796.63	3.5	6.9	6.9	13.7
3	7250	749.99	3.7	7.3	7.3	14.5
3	7500	704.11	3.9	7.8	7.8	15.5
3	7750	658.99	4.2	8.3	8.3	16.5
3	8000	614.64	4.5	8.9	8.9	17.7
3	8250	571.05	4.8	9.6	9.6	19.1
3	8500	528.23	5.2	10.4	10.4	20.6
3	8750	486.17	5.7	11.3	11.3	22.4
3	9000	444.87	6.2	12.4	12.4	24.5
3	9250	404.34	6.8	13.6	13.6	26.9
3	9500	364.57	7.5	15.1	15.1	29.9
3	9750	325.56	8.4	16.9	16.9	33.4
3	10000	287.32	9.6	19.1	19.1	37.9
3	10250	249.84	11.0	22.0	22.0	43.6
3	10500	213.13	12.9	25.8	25.8	51.1
3	10750	177.18	15.5	31.0	31.0	61.5
3	11000	141.99	19.4	38.7	38.7	76.7
3	11250	107.57	25.6	51.1	51.1	Range
3	11500	73.91	37.2	74.4	74.4	Range
3	11750	41.01	Irr	Range	Range	Range
3	12000	8.88	Range	Range	Range	Range

Nellis Atmosphere

Atm	Slant Range	Irradiance	Aim 1	Aim 2	Aim 3	Aim 4
4	2000	1975.97	1.4	2.8	2.8	5.5
4	2250	1914.06	1.4	2.9	2.9	5.7
4	2500	1852.90	1.5	3.0	3.0	5.9
4	2750	1792.51	1.5	3.1	3.1	6.1
4	3000	1732.88	1.6	3.2	3.2	6.3
4	3250	1674.02	1.6	3.3	3.3	6.5
4	3500	1615.92	1.7	3.4	3.4	6.7
4	3750	1558.59	1.8	3.5	3.5	7.0
4	4000	1502.01	1.8	3.7	3.7	7.3
4	4250	1446.21	1.9	3.8	3.8	7.5
4	4500	1391.16	2.0	4.0	4.0	7.8
4	4750	1336.88	2.1	4.1	4.1	8.1
4	5000	1283.36	2.1	4.3	4.3	8.5
4	5250	1230.61	2.2	4.5	4.5	8.8
4	5500	1178.62	2.3	4.7	4.7	9.2
4	5750	1127.40	2.4	4.9	4.9	9.7
4	6000	1076.93	2.6	5.1	5.1	10.1
4	6250	1027.24	2.7	5.4	5.4	10.6
4	6500	978.30	2.8	5.6	5.6	11.1
4	6750	930.13	3.0	5.9	5.9	11.7
4	7000	882.72	3.1	6.2	6.2	12.3
4	7250	836.08	3.3	6.6	6.6	13.0
4	7500	790.20	3.5	7.0	7.0	13.8
4	7750	745.09	3.7	7.4	7.4	14.6
4	8000	700.73	3.9	7.8	7.8	15.5
4	8250	657.15	4.2	8.4	8.4	16.6
4	8500	614.32	4.5	9.0	9.0	17.7
4	8750	572.26	4.8	9.6	9.6	19.0
4	9000	530.96	5.2	10.4	10.4	20.5
4	9250	490.43	5.6	11.2	11.2	22.2
4	9500	450.66	6.1	12.2	12.2	24.2
4	9750	411.66	6.7	13.4	13.4	26.5
4	10000	373.41	7.4	14.7	14.7	29.2
4	10250	335.94	8.2	16.4	16.4	32.4
4	10500	299.22	9.2	18.4	18.4	36.4
4	10750	263.27	10.4	20.9	20.9	41.4
4	11000	228.08	12.1	24.1	24.1	47.7
4	11250	193.66	14.2	28.4	28.4	56.2
4	11500	160.00	17.2	34.4	34.4	68.1
4	11750	127.11	21.6	43.3	43.3	85.7
4	12000	94.97	29.0	57.9	57.9	Range

Davis-Monthan/Hail Saudi Arabia Atmosphere

Gibraltar Atmosphere

Atm	Slant Range	Irradiance	Aim 1	Aim 2	Aim 3	Aim 4
7	2000	2289.52	1.2	2.4	2.4	4.8
7	2250	2227.60	1.2	2.5	2.5	4.9
7	2500	2166.45	1.3	2.5	2.5	5.0
7	2750	2106.06	1.3	2.6	2.6	5.2
7	3000	2046.43	1.3	2.7	2.7	5.3
7	3250	1987.57	1.4	2.8	2.8	5.5
7	3500	1929.47	1.4	2.9	2.9	5.6
7	3750	1872.13	1.5	2.9	2.9	5.8
7	4000	1815.56	1.5	3.0	3.0	6.0
7	4250	1759.75	1.6	3.1	3.1	6.2
7	4500	1704.71	1.6	3.2	3.2	6.4
7	4750	1650.43	1.7	3.3	3.3	6.6
7	5000	1596.91	1.7	3.4	3.4	6.8
7	5250	1544.16	1.8	3.6	3.6	7.1
7	5500	1492.17	1.8	3.7	3.7	7.3
7	5750	1440.94	1.9	3.8	3.8	7.6
7	6000	1390.48	2.0	4.0	4.0	7.8
7	6250	1340.78	2.1	4.1	4.1	8.1
7	6500	1291.85	2.1	4.3	4.3	8.4
7	6750	1243.68	2.2	4.4	4.4	8.8
7	7000	1196.27	2.3	4.6	4.6	9.1
7	7250	1149.63	2.4	4.8	4.8	9.5
7	7500	1103.75	2.5	5.0	5.0	9.9
7	7750	1058.63	2.6	5.2	5.2	10.3
7	8000	1014.28	2.7	5.4	5.4	10.7
7	8250	970.69	2.8	5.7	5.7	11.2
7	8500	927.87	3.0	5.9	5.9	11.7
7	8750	885.81	3.1	6.2	6.2	12.3
7	9000	844.51	3.3	6.5	6.5	12.9
7	9250	803.98	3.4	6.8	6.8	13.5
7	9500	764.21	3.6	7.2	7.2	14.3
7	9750	725.20	3.8	7.6	7.6	15.0
7	10000	686.96	4.0	8.0	8.0	15.9
7	10250	649.48	4.2	8.5	8.5	16.8
7	10500	612.77	4.5	9.0	9.0	17.8
7	10750	576.82	4.8	9.5	9.5	18.9
7	11000	541.63	5.1	10.2	10.2	20.1
7	11250	507.21	5.4	10.8	10.8	21.5
7	11500	473.55	5.8	11.6	11.6	23.0
7	11750	440.65	6.2	12.5	12.5	24.7
7	12000	408.52	6.7	13.5	13.5	26.7

Bibliography

Albertine, John R. "History of navy HEL technology development and systems testing" Proceedings of SPIE - The International Society for Optical Engineering v4632, 2002

Anderson, Colin M. *Generalized Weapon Effectiveness Modeling*. MS thesis, Naval Postgraduate School Monterey CA, June 2004

Azar, Maurice C. *Assessing the Treatment of Airborne Tactical High Energy Lasers in Combat Simulations.* MS thesis, Air Force Institute of Technology Dayton OH, May 2003

Chen, Zongli and others. *Measurement of Energy Distribution and Analysis of Hazard Probability of Long-Distance Laser Irradiation*. Wright Patterson AFB, Ohio: National Air Intelligence Center, 1996

Cook, Michael T. *Improving the Estimation of the Military Worth of the Advanced Tactical Laser Through Simulation Aggregation.* MS thesis, Air Force Institute of Technology Dayton OH, March 2004

HELEEOS User's Guide v1.2, Air Force Institute of Technology Center for Directed Energy

"History of the ABL" excerpt from unpublished article. n. pag. http://www.boeing.com/special/abl/history/

Latham, W.P., Beraun, J.E. "Laser effects research and modeling to support high energy laser systems" Proceedings of SPIE - The International Society for Optical Engineering v4376, 2001

Lee, David and others. *Analytic methods for tactical air warfare: air campaign and high-energy laser propagation analysis* Mclean, Virginia: Logistics Management Institute, 2004.

Link, Donald J. (SAIC); John, Richard St.. "Simulation and modeling of high energy laser systems" Proceedings of SPIE - The International Society for Optical Engineering, v 5414, 2004

Mendelson, Frank. <u>Schaum's Outline of Calculus,</u> 4th edition, 1999 McGraw-Hill

Newberry, Russell D. *Evaluation of Air-to-Ground Weapon Delivery Systems Performance.* TM 80-1 SA. Patuxent River, Maryland: Naval Air Test Center, 1980

Perram, Glen P. Marciniak, Michael A.; Goda, Matthew "High energy laser weapons: technology overview" Proceedings of SPIE - The International Society for Optical Engineering, v 5414, 2004

Shannon, R.E., (1975a), Systems Simulation: The Art and Science, Englewood Cliffs, N.J.: Prentice-Hall, Inc.

Shwartz, Josef. "Tactical High Energy Laser", Proceedings of SPIE - The International Society for Optical Engineering. v4632, 2002

Thompson, Scott. "Initial Answers" Electronic Message. 21 April 2005.

Tyson, Robert K. Principles of Adaptive Optics (2nd Edition). San Diego: Academic Press, 1998.

REPORT DOCUMENTATION PAGE	*Form Approved* *OMB No. 074-0188*

The public reporting burden for this collection of information is estimated to average 1 hour per response, including the time for reviewing instructions, searching existing data sources, gathering and maintaining the data needed, and completing and reviewing the collection of information. Send comments regarding this burden estimate or any other aspect of the collection of information, including suggestions for reducing this burden to Department of Defense, Washington Headquarters Services, Directorate for Information Operations and Reports (0704-0188), 1215 Jefferson Davis Highway, Suite 1204, Arlington, VA 22202-4302. Respondents should be aware that notwithstanding any other provision of law, no person shall be subject to an penalty for failing to comply with a collection of information if it does not display a currently valid OMB control number.
PLEASE DO NOT RETURN YOUR FORM TO THE ABOVE ADDRESS.

1. REPORT DATE *(DD-MM-YYYY)*	**2. REPORT TYPE**	**3. DATES COVERED** *(From – To)*
13/06/2005	Master's Thesis	August 2003 – May 2005

4. TITLE AND SUBTITLE CATEGORIZING HIGH ENERGY LASER EFFECTS FOR THE JOINT MUNITIONS EFFECTIVENESS MANUAL	**5a. CONTRACT NUMBER** **5b. GRANT NUMBER** **5c. PROGRAM ELEMENT NUMBER**
6. AUTHOR(S) Markham James A, Captain, USAF	**5d. PROJECT NUMBER** **5e. TASK NUMBER** **5f. WORK UNIT NUMBER**
7. PERFORMING ORGANIZATION NAMES(S) AND ADDRESS(S) Air Force Institute of Technology Graduate School of Engineering and Management (AFIT/EN) 2950 Hobson Way, Building 640 WPAFB OH 45433-8865	**8. PERFORMING ORGANIZATION REPORT NUMBER** AFIT/GOR/ENS/05-11
9. SPONSORING/MONITORING AGENCY NAME(S) AND ADDRESS(ES) N/A	**10. SPONSOR/MONITOR'S ACRONYM(S)** **11. SPONSOR/MONITOR'S REPORT NUMBER(S)**

12. DISTRIBUTION/AVAILABILITY STATEMENT

APPROVED FOR PUBLIC RELEASE; DISTRIBUTION UNLIMITED.

13. SUPPLEMENTARY NOTES

14. ABSTRACT

With the high risk and cost in fielding High Energy Laser (HEL) weapon systems, the development process must include computer simulation models of weapon system performance from the engineering level up to predicting the military worth of employing specific systems in a combat scenario. This research effort focuses on defining how to measure lethality for HEL weapons in an Advanced Tactical Laser (ATL) scenario. In order to create an effective measure for direct comparison between the emerging laser weapon system and existing conventionally delivered weapons, lase time in seconds is presented as a measure comparable to rounds required to cause the desired effect at the target. An examination of input parameters which influence the output power of the laser at the target and thus the required lase time is presented with particular attention being paid to atmospheric conditions and vulnerable bucket size. Results include output tables providing the lase time required for melt-through of a set of generic truck-type vehicular ground target aimpoints.

15. SUBJECT TERMS

Laser, Vulnerability, Effectiveness, JMEM, Joint Munitions Effectiveness Manual

16. SECURITY CLASSIFICATION OF:			**17. LIMITATION OF ABSTRACT**	**18. NUMBER OF PAGES**	**19a. NAME OF RESPONSIBLE PERSON**
a. REPORT	**b. ABSTRACT**	**c. THIS PAGE**			J.O. Miller, PhD
U	U	U	UU	106	**19b. TELEPHONE NUMBER** *(Include area code)* (937) 255-6565, ext 4326 (john.miller@afit.edu)

Standard Form 298 (Rev. 8-98)
Prescribed by ANSI Std. Z39-18